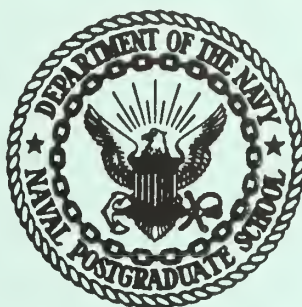


UNITED STATES NAVAL POSTGRADUATE SCHOOL



THESIS

A SIX LEVEL PROGNOSTIC-DIAGNOSTIC
SOLUTION PROCEDURE WITH A NEW
APPROACH IN MODELING OF BOUNDARY
LAYER FRICTIONAL EFFECTS

by

William Loynes Danforth

and

Paul Peter Kalinyak

June 1968

THESIS
D1477

This document is subject to special export controls and each transmittal to foreign government or foreign nationals may be made only with prior approval of the U. S. Naval Postgraduate School.

LIBRARY
NAVAL POSTGRADUATE SCHOOL
MONTEREY, CALIF. 93940

[REDACTED]

A SIX LEVEL PROGNOSTIC-DIAGNOSTIC
SOLUTION PROCEDURE WITH A NEW
APPROACH IN MODELING OF BOUNDARY
LAYER FRICTIONAL EFFECTS

by

William Loynes Danforth
Lieutenant, United States Navy
B. A., Dartmouth College, 1960

and

Paul Peter Kalinyak
Lieutenant Commander, United States Navy
B. S., University of Pittsburgh, 1953

Submitted in partial fulfillment of the
requirements for the degree of

MASTER OF SCIENCE IN METEOROLOGY

from the

NAVAL POSTGRADUATE SCHOOL
June 1968

0 0 0 0 0

D. 14-17
C. 2
1/8

ABSTRACT

A six-level baroclinic forecast model suitable for numerical prognosis was devised. This model includes vertical motion due to large-scale orographic and eddy-stress effects. The model was programmed in Fortran IV language and applied to a test case based upon initial data fields for 1200GMT, 15 December 1967. A convergent 36-hour forecast was produced. Comparisons were made with the verifying analyses at 12-hourly intervals.

TABLE OF CONTENTS

	Page
LIST OF TABLES	5
LIST OF ILLUSTRATIONS	7
LIST OF SYMBOLS	9
ACKNOWLEDGEMENTS	11
SECTION	
1. Introduction	13
2. Inclusion of large-scale friction in the vorticity equation	16
3. Derivation and solution of the diagnostic omega equation	21
4. Solution of the prognostic equation	25
5. Forecast verification results	28
6. Remarks and conclusions	31
BIBLIOGRAPHY	68
APPENDIX A: Computation of Terrain Pressure	70
APPENDIX B: Treatment of Vertical Derivatives	72
APPENDIX C: Treatment of Horizontal Derivatives	75
APPENDIX D: Computation of Static Stability Parameter	77
APPENDIX E: Procedure for 100-mb Height Extrapolation	79
APPENDIX F: FORTRAN IV Program	80

LIST OF TABLES

TABLE		PAGE
1.	F(p) Values for Use in Equation (14)	33
	a. Gradient level assumed as 850 mb	
	b. Gradient level assumed as 700 mb	
2.	Root Mean Square Error Results	34

LIST OF ILLUSTRATIONS

FIGURE		PAGE
1.	Level Diagram	35
2.	Grid Map	36
3a.	Flow Diagram	37
3b.	Flow Diagram (continued)	38
4a.	Tape 11 Record Layout	39
4b.	Disks 12 and 13 Record Layout	40
4c.	Tape 14 Record Layout	41
5.	12Z 15 December 67 1000-mb Analysis	42
6.	12Z 15 December 67 500-mb Analysis	43
7.	12Z 15 December 67 300-mb Analysis	44
8.	00Z 16 December 67 1000-mb Analysis	45
9.	00Z 16 December 67 500-mb Analysis	46
10.	00Z 16 December 67 300-mb Analysis	47
11.	Verifying Time (VT) 00Z 16 December 67 1000-mb 12-HR. FCST.	48
12.	VT 00Z 16 December 67 500-mb 12-HR. FCST.	49
13.	VT 00Z 16 December 67 300-mb 12-HR. FCST.	50
14.	12Z 16 December 67 1000-mb Analysis	51
15.	12Z 16 December 67 500-mb Analysis	52
16.	12Z 16 December 67 300-mb Analysis	53
17.	VT 12Z 16 December 67 1000-mb 24-HR. FCST.	54
18.	VT 12Z 16 December 67 500-mb 24-HR. FCST.	55
19.	VT 12Z 16 December 67 300-mb 24-HR. FCST.	56

20.	00Z 17 December 67 1000-mb Analysis	57
21.	00Z 17 December 67 500-mb Analysis	58
22.	00Z 17 December 67 300-mb Analysis	59
23.	VT 00Z 17 December 67 1000-mb 36-HR. FCST.	60
24.	VT 00Z 17 December 67 500-mb 36-HR. FCST.	61
25.	VT 00Z 17 December 67 300-mb 36-HR. FCST.	62
26.	VT 00Z 16 December 67 850-mb 12-HR. FCST. ω -Field	63
27.	VT 00Z 16 December 67 700-mb 12-HR. FCST. ω -Field	64
28.	VT 00Z 16 December 67 500-mb 12-HR. FCST. ω -Field	65
29.	VT 00Z 16 December 67 300-mb 12-HR. FCST. ω -Field	66
30.	VT 00Z 16 December 67 200-mb 12-HR. FCST. ω -Field	67
31.	Finite Differencing Grid	76

LIST OF SYMBOLS

Symbol		Units
J	Jacobian operator	m^{-2}
∇^2	Laplacian operator	m^{-2}
∇^2	Finite-difference Laplacian operator	m^{-2}
∇	Del operator	m^{-1}
ψ	Stream function for non-divergent motion	$m^2 sec^{-1}$
χ	Velocity potential for irrotational motion	$m^2 sec^{-1}$
$\nabla\psi$	Vector stream velocity	$m sec^{-1}$
ζ	Absolute vorticity	sec^{-1}
f	Coriolis parameter	sec^{-1}
j	Relative vorticity	sec^{-1}
ω	Terrain and friction-induced vertical velocity	$mb sec^{-1}$
ω_f	Friction-induced vertical velocity	$mb sec^{-1}$
ω_T	Terrain-induced vertical velocity	$mb sec^{-1}$
ω_{LO}	Terrain and friction-induced vertical velocity at gradient level	$mb sec^{-1}$
ω	Vertical velocity not including terrain and frictional effects	$mb sec^{-1}$
σ	Static stability parameter	$m^2 sec^{-2} mb^{-2}$
∇g_F	Vector geostrophic wind at gradient level	$m sec^{-1}$
V_{gF}	Geostrophic wind speed at gradient level	$m sec^{-1}$
P_T	Terrain pressure	mb

Symbol		Units
p_F	Pressure at gradient level	mb
g	Acceleration due to gravity	$m \text{ sec}^{-2}$
ρ	Density at gradient level	$kg \text{ m}^{-3}$
C_d	Drag coefficient	
z	Geometric height	m
Φ	Geopotential height	$m^2 \text{ sec}^{-2}$
z_o	Roughness parameter	m
R_d	Gas constant	joules $kg^{-1} K^{-1}$
C_p	Specific heat of air at constant pressure	joules $kg^{-1} K^{-1}$
z_T	Terrain height	m

ACKNOWLEDGEMENTS

The authors would like to take this opportunity to express their appreciation to those who have assisted in the preparation of this investigation. The authors are especially grateful to their advisor, Professor Frank L. Martin, for his invaluable guidance and advice in the application of the theoretical model to this numerical study; to Mr. Leo C. Clarke of the Fleet Numerical Weather Central, Monterey, for providing the initial and verifying data; and to Mr. Ron Brunell, for converting the data to a form usable on the IBM 360, also goes the authors' appreciation.

1. Introduction

One of the most successful numerical forecasting procedures is that of F. G. Shuman (1967) and his co-workers at the National Meteorological Center. This is a very sophisticated forecast scheme involving the primitive equations of motion. From the progressive improvement of NMC forecast skill-score measures, there seems to be little question that the NMC approach must be regarded as the direction of ultimate progress in the field of objective prognosis.

One of the possible demerits to the use of the NMC system, at least in its present transitional stage, is the vast amount of sophisticated computer-time and memory required. Secondly, it employs the vertical σ_T coordinate system¹, where σ_T (tropospheric σ) is defined as

$$\sigma_T = \frac{p - p_T}{p_T^* - p_T} \quad (1)$$

where

p_T = pressure at terrain

p = pressure at $\sigma_T = 0, 1/3, 2/3, 1$

p^* = pressure at the tropopause
(assumed to be a material surface).

In addition to the short time-step used in each NMC prediction iteration, a considerable amount of time is spent in interpolation from standard pressure levels (e.g., Fig. 1) to the σ surfaces for the purposes of the prognosis. This is followed by a final interpolation back to standard pressure-surface levels. Thus, it was felt here that an attempt, using vorticity methods, to initiate a quasi-hemispheric multi-level

¹This description of the Shuman σ -model is not that of his most recent model (1967) which includes, in addition, some stratospheric layers.

forecast system could be of real advantage to the "small-shop" forecaster.

In this attempt the conventional FNWC-NMC grid is used, but at least some of the terrain effects embodied in the Shuman scheme are retained, even though the vorticity equation approach is used.

In this method one expresses the horizontal wind by means of its usual Helmholtz expression.

$$\mathbf{V} = \mathbf{k} \times \nabla \psi + \nabla \chi \quad (2)$$

Furthermore, if neither friction nor heat sources are to be considered, temporarily at least, Arakawa (1962) and others have shown that the following pair of equations represent an energy-conserving system over a closed mass of air:

$$\nabla^2 \psi_t + J(\psi, \eta) + \nabla \chi \cdot \nabla f = f \frac{\partial \omega}{\partial p} \quad (3)$$

$$\nabla \cdot f \nabla \psi = \nabla^2 \Phi \quad (4)$$

The use of the linear balance equation (4) would have its usual effect of eliminating gravity waves, initially at least. If terrain-induced friction, in its broadest sense, is to be introduced, its effect would impinge upon eq. (3), effecting changes primarily upon the χ field, and to a lesser extent upon the ψ field, since the balance equation is considered to be in effect throughout the forecast period. The local time derivative form of (4),

$$\nabla \cdot f \nabla \psi_t = \nabla^2 \Phi_t \quad (5)$$

is to be used in deriving the omega equation in section 3.

Because of the boundary layer model which is adopted in section 2, it is expected that point and/or area sources of vorticity will be

present within the grid; therefore, the prognostic step at any time requires a continuous process of lateral diffusion, within the diffusion limits suggested by Grimmer (1941), by means of a term of the form $K \nabla^2 J$ to be added to the right side of (3). Diffusion also serves to prevent eq. (3) from developing computational instability when frictional considerations are injected, provided $K \frac{\Delta t}{(\Delta x)^2} < \frac{1}{2}$ [Richtmyer and Morton (1967)]. Here Δt is the time increment, and Δx is the grid-mesh size.

2. Inclusion of large-scale friction in the vorticity equation

If one retains the relatively simple Arakawa vorticity equation, while introducing friction-induced vertical motion, the resultant modified equation would, in the absence of orography, assume the form:

$$\nabla^2 \psi_t + J(\psi, \eta) + \nabla X \cdot \nabla f = f \frac{\partial \omega}{\partial p} - g \frac{\partial}{\partial p} (K \cdot \nabla \times \mathcal{U}) + K \nabla^2 J \quad (6)$$

Still considering a turbulent boundary layer over a level-earth surface, the second term on the right side of (6) is expressible, in terms of a turbulence-induced vertical motion Ω , by the identity

$$f \frac{\partial \Omega}{\partial p} = -g \frac{\partial}{\partial p} (K \cdot \nabla \times \mathcal{U}) \quad (7)$$

If the Cressman approach (1960) to the parameterization of the frictional stress at gridpoints is employed, one may write

$$\mathcal{U} = -\rho C_d V_{gF} V_{gF} \quad (8)$$

where C_d is actually taken from seasonal values at gridpoints after Kung (1963). At the top of the frictional boundary layer (indexed as $F=1$ or 2 in Fig. 1) integration of $\Omega(p)$ gives the eddy-stress vertical motion component Ω_f as follows:

$$\Omega_f = -\frac{g}{f} K \cdot \nabla X (\rho C_d V_{gF} V_{gF}) \quad (9)$$

which, after expansion, leads to

$$\Omega_f = -\frac{g}{f} \rho [C_d V_{gF} J_{gF} + \frac{g}{f} \nabla (C_d V_{gF}) \cdot \nabla Z_F] \quad (10)$$

In eqs. (8) and (9) the Kung drag coefficients are applied in connection with the geostrophic wind V_{gF} at the top of the planetary boundary layer.

If we revert now to a terrain-variable earth, another obvious term arises when orography is introduced, namely

$$\Omega_T = \left(\frac{dp}{dt} \right)_T = \frac{\partial p}{\partial t} + \mathbf{V} \cdot \nabla p_T \doteq \mathbf{V}_{gF} \cdot \nabla p_T \quad (11)$$

This version of Ω_T is then combined with Ω_f of (9) so that the resultant maximum terrain-induced vertical velocity to be applied at the boundary-layer top is

$$\Omega_{LO} = \Omega_T + \Omega_f \quad (12)$$

where Ω_{LO} is to be defined as:

$$\Omega_{LO} = \left\{ \mathbf{V}_{gF} \cdot \nabla p_T - \frac{g}{f} \rho [C_d \mathbf{V}_{gF}]_{gF} + \frac{g}{f} \nabla (C_d \mathbf{V}_{gF}) \cdot \nabla Z_F \right\} \quad (13)$$

The term $\mathbf{V}_{gF} \cdot \nabla p_T$ qualitatively accounts for upward motion on the windward side of a mountain range and the reverse effect on the leeward side. In the computation of this term, actual values of pressure at terrain have been computed from consideration of the Berkofsky-Bertoni station elevations (1955) employing a method by means of which the terrain pressure is hydrostatically computed from the thermal character of the isobaric layer in which the terrain is embedded (see Appendix A).

For the most part, the Berkofsky-Bertoni smoothed station elevations over North America do not exceed 9000 feet. On the Asiatic continent, however, derived terrain pressures as low as 500 mb are encountered. In this regard there is a dilemma: At what level should \mathbf{V}_{gF} be considered representative when terrain reaches such high levels? If p_T lies between 850 and 700 mb a choice of planetary boundary layer at 700 mb would appear perfectly reasonable. If p_T

exceeds 850 mb by 100 mb or so, the planetary boundary layer could reasonably be taken at 850 mb.

Some upper limit to the magnitude of the \mathbf{V}_{gF} vector used in Ω_T was considered appropriate in view of the calibration of Kung's sea-level geostrophic drag coefficients. For example, even with $p_T \approx 500$ mb, it is reasonable to consider that the effective updraft component need not exceed that of the 700-mb geostrophic wind over the generally rough terrain involved. Also, for simultaneous use of both Ω_T and Ω_F in (12), it is desirable to arrive objectively at a mutually compatible gradient level. In view of these considerations, the following scheme was devised to delineate the boundary layer: if p_T is greater than 875 mb, p_F (the boundary layer pressure) is chosen as 850 mb; if p_T is equal to or less than 875 mb, p_F is chosen as 700 mb. The choice of the planetary boundary layer which employs gridpoint wind data at either 850 mb or 700 mb is one of the simplifying features of the general frictional model introduced here. Because of the preservation of the orographic term, $\mathbf{V}_{gF} \cdot \nabla p_T$, with \mathbf{V}_{gF} equal either to \mathbf{V}_{gF} (850) or to \mathbf{V}_{gF} (700), it is felt that some of the main physical aspects of the variable atmospheric boundary layer are being preserved by the model, while retaining an element of convenience in a 6-level forecast model. Furthermore a recent study by Graham (1968) indicates that Kung's drag coefficient gives consistently smaller values than those proposed by Cressman; so their use in (8) and (9) appears reasonable with these geostrophic winds at the selected tops of the atmospheric boundary layer.

The significance of the specification of the top of the atmospheric boundary layer (A.B.L.) is that this level is conventionally associated

with the maximum frictional vertical motion [c.f. Haltiner et al. (1963), Krishnamurti (1968)] which then decays in some generally exponential manner on either side of this level. Thus, for $p \neq p_F$, the existence of a frictionally-induced vertical velocity $\Omega(p)$ may be postulated, in accordance with (13), as

$$\Omega(p) = F(p) \Omega_{L_0} \quad (14)$$

Above the A.B.L. an analytic function $F_a(p)$ for $\Omega(p)$ is chosen so as to imply that

$$\left. \begin{aligned} F_a(100) &= 0 \\ F_a(p_F) &= 1 \end{aligned} \right\} \quad (15)$$

and that $F_a(p)$ is a decay factor which decreases realistically with decreasing pressure. The choice of $F_a(p)$ was made with a careful attempt at fitting the mean vertical profiles of frictionally induced $\Omega(p)$ depicted by Haltiner et al. (1963) in the case p_F equal to 850 mb. The analytic function selected for $F_a(p)$ was

$$F_a(p) = \left[1 - \frac{\ln p/p_F}{\ln 100/p_F} \right]^3, \quad (16)$$

which decreases in a closely similar manner to that shown in synoptic evidence by Haltiner et al. (1963), and with that alluded to by Estoque (1957). Values of $F_a(p)$ are shown in Tables 1a and 1b.

For elevations below the A.B.L., there is no published data to draw upon. Here it was desired to apply once more the limiting boundary conditions similar to (15) for $p = 1000$ mb and $p = p_F$. It is also desirable to consider a function $F_b(p)$ for multiplicative association with Ω_{L_0} with a smaller rate of variation with p/p_F than is the case with $F_a(p)$. Such a function, somewhat analogous to (16) and subject

to the above constraints as (16), was chosen by limiting the bracketed expression in (16) to the exponent 2:

$$F_b(p) = \left[1 - \frac{\ln \frac{p/p_E}{1000/p_E}}{\ln \frac{p/p_E}{1000/p_E}} \right]^2 \quad (17)$$

The values of $F_b(p)$ are also in Tables 1a and 1b. It is evident that the formulation of $f \frac{\partial \Omega}{\partial p}$ in (7), which will appear on the right side of (6), depends only upon $\frac{\partial F}{\partial p}$. The finite-difference derivative with respect to pressure will in turn depend upon the scheme adopted for the finite-differencing of ω in the vertical, a topic to be discussed in connection with the solution of the omega equation. The distinction between ω and Ω is that the former represents the result of partitioning the total vertical motion into a component free of frictional effects, whereas Ω is the composite vertical motion resulting from large-scale friction. Note that the net frictional divergence in any column (which may include terrain) extending from the 1000-mb level to the 100-mb level is designed to be zero. Also since the lateral diffusion $K \nabla^2 \}$ is defined to be zero on the octagonal grid boundary, eqs. (4) and (6) still represent an energy-preserving system of equations in an adiabatic atmosphere.

3. Derivation and solution of the diagnostic omega equation

In order to deduce the numerical solution of (6) for ψ_t , it is clear that one requires values for $\frac{\partial(\omega+\Omega)}{\partial p}$ at all prognostic levels. To obtain these vertical derivatives the diagnostic omega equation must first be solved at levels $k = 2$ to 6 .

The omega equation is derived from a combination of the vorticity equation and the thermodynamic equation.

The vorticity equation, after Arakawa (1962), is now presented as

$$\nabla^2 \psi_t + \mathbf{V}_\psi \cdot \nabla \eta + \nabla \chi \cdot \nabla f - f \frac{\partial \omega}{\partial p} = f \frac{\partial \Omega}{\partial p} + K \nabla^2 J \quad (18)$$

Equation (18) is differentiated with respect to pressure and multiplied by f to give the form

$$f \nabla^2 \psi_{pt} + f \frac{\partial}{\partial p} (\mathbf{V}_\psi \cdot \nabla \eta) + f \nabla f \cdot \nabla \chi_p - f^2 \frac{\partial^2 \omega}{\partial p^2} = f^2 \left(\frac{\partial^2 F}{\partial p^2} \right) \Omega_{L_0} \quad (19)$$

The lateral diffusion term $K \nabla^2 J$ has been omitted, since its use will be reserved for (18). Use of the time-differentiated linear balance equation in (19) leads to

$$\nabla^2 \Phi_{pt} - \nabla f \cdot \nabla \psi_{pt} + f \frac{\partial}{\partial p} [J(\psi, \eta)] + f \nabla f \cdot \nabla \chi_p - f^2 \frac{\partial^3 \omega}{\partial p^3} = f^2 \frac{\partial^2 \Omega}{\partial p^2} \quad (20)$$

The adiabatic thermodynamic equation is given as

$$\frac{\partial \Phi_p}{\partial t} + \mathbf{V}_\psi \cdot \nabla \Phi_p + \nabla \chi \cdot \nabla \Phi_p + \sigma(\omega + \Omega) = 0 \quad (21)$$

where

$$\sigma = - \frac{R_d T}{p \theta} \frac{\partial \theta}{\partial p}$$

and σ is also expressible in terms of geopotential meters mb^{-2} (see Appendix D). Application of the Laplacian operator, ∇^2 , to each term of eq. (21) gives

$$\nabla^2 \Phi_{pt} + \nabla^2 [J(\psi, \Phi_p)] + \nabla^2 (\nabla \chi \cdot \nabla \Phi_p) + \nabla^2 (\sigma \omega + \sigma \Omega) = 0 \quad (22)$$

Then $\nabla^2 \Phi_{pt}$ can be eliminated from eqs. (20) and (22) by subtraction. Hence eq. (23) is derived:

$$\begin{aligned} \nabla^2 (\sigma \omega) + f^2 \frac{\partial^2 \omega}{\partial p^2} &= f \frac{\partial}{\partial p} J(\psi, \eta) - \nabla^2 [J(\psi, \Phi_p)] \\ &+ \nabla \frac{f^2}{2} \cdot \nabla \chi_p - \nabla^2 (\nabla \chi \cdot \nabla \Phi_p) - f^2 \frac{\partial^2 \Omega}{\partial p^2} - \nabla f \cdot \nabla \psi_{pt} - \nabla^2 \sigma \Omega \end{aligned} \quad (23)$$

Now, use of the approximations,

$$\nabla f \cdot \nabla \psi_{pt} \doteq \frac{\nabla f \cdot \nabla \Phi_{pt}}{\bar{f}}, \quad \nabla \frac{f^2}{2} \cdot \nabla \chi_p \ll f \frac{\partial}{\partial p} J(\psi, \eta) \quad (24)$$

together with del operator applied to (21) leads to eq. (25):

$$\nabla f \cdot \nabla \psi_{pt} \doteq - \frac{\nabla f}{\bar{f}} \cdot \left[\nabla \{ J(\psi, \Phi_p) + \nabla \chi \cdot \nabla \Phi_p + \sigma (\omega + \Omega) \} \right] \quad (25)$$

Hence, the final form of the diagnostic omega equation is

$$\begin{aligned} \nabla^2 (\sigma \omega) + f^2 \frac{\partial^2 \omega}{\partial p^2} &= f \frac{\partial}{\partial p} [J(\psi, \eta)] - \nabla^2 [J(\psi, \Phi_p)] - \nabla^2 (\nabla \chi \cdot \nabla \Phi_p) \\ &- f^2 \frac{\partial^2 \Omega}{\partial p^2} + \frac{\nabla f}{\bar{f}} \cdot \left[\nabla \{ J(\psi, \Phi_p) + \nabla \chi \cdot \nabla \Phi_p + \sigma (\omega + \Omega) \} \right] - \nabla^2 \sigma \Omega \end{aligned} \quad (26)$$

Equation (26) now has terms involving partial derivatives in both the vertical and horizontal, requiring finite-difference schemes for these derivatives. Appendix B presents the scheme used for finite-differencing in the vertical, and Appendix C presents the scheme used for finite-differencing in the horizontal. Since ω appears in a vertical derivative in eq. (3), a solution of ω at every grid point for levels

k equal to 2 and 6 requires placing boundary conditions on omega at the topmost level (k = 7) and the bottommost level (k = 1) as well as at the lateral boundary of the octagonal grid (Fig. 2). These conditions

were that omega would be equal to zero at all of these boundaries.

Similarly, the Jacobian and Laplacian terms of all other parameters in (26) are set to zero at the lateral boundary. Once the terms of (26) are finite-differenced, we obtain a Helmholtz type of equation where

$$\nabla^2 \omega_k - B_k \omega_k = C_k + D_k \omega_{k-1} + E_k \omega_{k+1} . \quad (27)$$

Here C_k is the finite-differenced result of the right side of (26), and ω_{k-1} is presumed known. Equation (26) was solved by a 3-dimensional Liebmann relaxation scheme where the $(n + 1)$ th iterate for any point is given by

$$\omega_k^{n+1} = \omega_k^n + \frac{\lambda R^n}{4 + B_k} \quad (28)$$

Here λ is the over-relaxation coefficient and the residual R^n at the nth iteration is

$$R_k^n = \nabla^2 \omega_k^n - B_k \omega_k^n - C_k - D_k \omega_{k-1}^n - E_k \omega_{k+1}^{n-1} \quad (29)$$

In (28), (29), the superscript n indicates the nth iterate resulting from sequential Liebmann solution procedure. The convergence criterion imposed is that when R^n becomes less than $2 \cdot 10^{-6}$ for each grid-point, the iteration procedure ceases. For the first iteration ($t = 0$) all omegas of the right side of (29) were set to zero, and only the first 2 terms on the right side of eq. (26) were used to determine ω_k . When these omegas were computed for levels 2 through 6, then χ_k was determined by use of the equation of continuity in the form

$$\nabla^2 \chi_k = - \left[\frac{\partial (\omega + \Omega)}{\partial p} \right]_k \quad (30)$$

²In units of mb sec⁻¹

With a first determination of χ_k at the 5 central levels ($k = 2, \dots, 6$), the diagnostic equation could now be solved for a better ω and then a better χ . This ω - χ iterative procedure is repeated until, for all gridpoints, at the 5 central levels the omegas reach the convergent value.

For times other than $t = 0$, the full diagnostic equation is used even in the first iteration. The first guess for χ is that derived from the previous time step.

The above procedures apply identically for levels $k = 2, \dots, 6$. For the 1000-mb level a somewhat different procedure is necessary to obtain $\frac{\partial \omega}{\partial p}$ for use in connection with the continuity equation (30). This procedure is outlined in Appendix B. This same procedure also applies when obtaining $\frac{\partial \omega}{\partial p}$ for the prognostic step at 1000 mb.

4. Solution of the prognostic equation

With the vertical derivatives of omega and the divergent part of the wind now available for levels $k = 1$ through 6, the vorticity eq. (18) is now ready for solution for these same levels. With all the advective and divergent terms of this equation known at time t , and after finite-differencing and transposition, eq. (18) leads to the Poisson-type differential equation

$$\nabla^2 \left(\frac{\partial \psi}{\partial t} \right)_{i,j,k} = G(i,j,k) \quad (31)$$

where $G(i, j, k)$ represents the three-dimensional forcing function.

This equation is solvable one level at a time by assuming both that ψ_t at the octagonal boundary is zero and that all terms comprising $G(i, j, k)$ are also individually zero on the boundary. For solution of (31) one proceeds to a Liebmann two-dimensional iterative relaxation procedure, using successive iterates in the form

$$\psi_t^{n+1} = \psi_t^n + \frac{\lambda R^n}{4} \quad (32)$$

for any one level. Here, as in the relaxation process for ω , the superscript $n + 1$ refers to the $(n + 1)$ th iterative value, and the n -superscript refers to the n th iterative value. Again λ refers to the over-relaxation coefficient and the residual R is expressed as:

$$R^n = \nabla^2 \psi_t^n - G \quad (33)$$

This iterative procedure continues until the maximum residual at any iteration is less than the prescribed epsilon value, $\epsilon = 6.4 \times 10^{-11} \text{ sec}^{-2}$.

Because of the simplified method of determining the gradient level, and to take into account discontinuities in the A.B.L. occurring between

adjacent gridpoints, the term $K \nabla^2 \psi$ is included in (18) as a smoothing, or diffusion term. Several values of K were used with varying results. The initial value was $4.0 \times 10^5 \text{ m}^2 \text{ sec}^{-1}$, as suggested by Danard (1966). This resulted in extreme deepening of lows and building of highs. The value $4.0 \times 10^6 \text{ m}^2 \text{ sec}^{-1}$ was then attempted which gave the opposite effect, namely to flatten out systems excessively. Also lateral boundary difficulties became apparent with the larger smoothing coefficient. The next and final value chosen was $1.2 \times 10^6 \text{ m}^2 \text{ sec}^{-1}$ which, while perhaps not the optimum value, gave better verification at $t = 12$ hours. In accord with convergence requirements for a parabolic-type differential equation, the smoothing was applied to the ψ field of the time $t-1$ rather than time t .

With ψ_t ($t = 0$) computed initially, ψ for a 30 minute time-increment was determined by a forward time step, represented symbolically by

$$\psi' = \psi^0 + \psi_t^0 (\Delta t) \quad (34)$$

For the next time step, also for $\Delta t = 30$ minutes, a centered or leap-frog type time step was utilized with $m = 1$ in (35):

$$\psi^{m+1} = \psi^{m-1} + \psi_t^m (2 \Delta t) \quad (35)$$

For $m > 1$ all time steps were of the leap-frog type with $2 \Delta t = 2$ hours.

New values for the stream function were thus obtained at all levels up to 200 mb. These values were converted to heights by the solution of the balance equation. In order to obtain vertical derivatives of geopotential at 200 mb, and to obtain a more accurate stability parameter

$\mathcal{J}(200)$, it was deemed necessary to obtain a good estimate of the 100-mb height field (see \mathcal{J}_h in eq. D-6). This was accomplished by use of regression equations developed by Lea (1961), for details see Appendix E.

With forecast values of Z available for levels $k = 1$ to 7, further time steps could now be computed by the procedure described in the diagnostic section and this section.

5. Forecast verification results

As a preface to the discussion of the forecast verification results, the labeling of the maps (figs. 5-30) will be explained. All 1000-mb contours are labeled in whole meters and contours are drawn at every 60 meters. The 500- and 300-mb contours are labeled with the thousands digit dropped. (Thus a height of 5580 meters is labeled 580). The contours at these levels are drawn at every 120 meters. The isolines of vertical velocity are drawn with an interval of 2×10^{-3} millibars per second with the exception of the 200-mb level where contours are drawn at every 0.5×10^{-3} interval. Labels are millibars per second $\times 10^3$.

Although forecast maps were produced for 7 levels, only the 1000-, 500-, and 300-mb levels are presented in order to maintain the discussion at a reasonable level. These forecasts are for 12-hour intervals out to 36 hours.

The test case chosen, 1200Z 15 Dec. 1967, was one which was recent and thus readily available and one which shows extensive deepening and movement of pressure systems at most levels.

The initial 1000-mb analysis shows an inactive 60-meter low center over Southern and Baja California which in 36 hours deepened to a minus 120-meter contour and moved to the Colorado area. The 36-hour forecast did not verify the deepening; however, a trough-type intrusion into this area has occurred in the same general area. This low system aloft had a near vertical closed circulation throughout the atmosphere, and had a movement to the northeast of 600 nautical miles, with slight deepening at the 300-mb level. The upper level forecast moved this system northward 150 nautical miles and filled it considerably.

In the North Atlantic a low system of minus 120-meters, with troughing to the WNW at 1000 mb at initial time, split into two minus 120-meter systems in 36 hours: one positioned near the original low and the second positioned just west of Newfoundland. The 36-hour forecast for this level shows a minus 240-meter contour just to the northwest of Newfoundland. The initial system had a WNW tilt with height and a closed 8640-meter contour centered at 52N-65W at the 300-mb level, which in 36 hours deepened to a 8520-meter contour at 47N-60W. For the forecast system at 300-mb the model verified on position but filled the low center to a 8700-meter contour. At the 500-mb level the prognosis verified with respect to position and height.

Initially, east of Hokkaido, Japan, there was a 1000-mb low center with a minus 60-meter contour. This low deepened rapidly for the first 12 hours and then the deepening subsided. In 36 hours it was positioned east of the Kamchatka Peninsula with a closed minus 180-meter contour. The surface forecast position verified exactly, but the forecast deepened the system too much. The initial 300-mb map indicated that a short wave trough was associated with this surface system; in 36 hours it had moved NE an amount consistent with that of the surface system while leaving a stationary long wave secondary trough west of Kamchatka. Both of these 300-mb trough features verified quite well.

At the initial time, a surface low center (minus 120-meter contour), was located off the central coast of Norway. It traveled ESE to Western Russia, maintaining its initial contour height. The model captured this movement almost exactly but again indicated too much low-level deepening. At the upper levels a trough associated with this system moved ESE to a position over the Baltic Sea in 36 hours. This

trough movement was captured well by the model at both the 500- and 300-mb levels and the height of the 500-mb level also verified.

Centered at 67N-85E at the 1000-mb level at the initial time was a minus 180-meter contour. This low filled to a minus 60-meter contour in 36 hours and was positioned at 74N-110E in 36 hours. The model missed this system badly by deepening it throughout the 36-hour period to a minus 240 meter contour positioned at 72N-90E, about 250 miles to the west of the actual position. This system at 500 mb was only forecast to deepen slightly. This slight deepening and position was verified by the 00Z 17 December analysis.

After 36 hours, with the exception of the low system over the central United States, there was generally good agreement in the 1000-mb low systems' positions; however, the model tested produced excessive deepening in some of the surface low systems by an extent of the order of 15 mb. At the upper levels one may easily identify comparable systems but again the position of systems verified better than the intensities; and the 500-mb systems verified better than those of the 300-mb level on both intensity and position. Table 2 presents the pillow and root mean square error for all 6 levels at 12-hourly intervals based on all internal gridpoints.

Figures 26 to 30 show the vertical-motion or ω charts produced at $t = 12$ hours, namely at 00Z, 16 December 1967 for the levels 850, 700, 500, 300, and 200 mb. It is noteworthy that maximum values seem to be closely aligned in the vertical with extreme maximum values occurring generally at 500 mb. However, ω_{300} was in general closer in magnitude to ω_{500} than was ω_{700} . The extreme magnitudes computed were near $6.0 \times 10^{-3} \text{ mb sec}^{-1}$ at 500 mb, which are close to values reported in a case study by Krishnamurti (1968).

6. Remarks and conclusions

Due to lack of sufficient core space it was not possible to maintain all necessary fields for one time step in core. The choice was made to maintain only the information for a triad of levels at one time. This necessitated a large amount of reading from and writing on direct-access storage devices as is evidenced by the FORTRAN program. This increased the running time of the program considerably. In order to limit the continuous running time of the program, the 36-hour forecast was produced in 3 runs of 12 hours each. The current values of height, ω , χ , ψ , as well as the ψ at the preceding time step were stored on disk and these values were read to begin the first time step of the next run. (For the layout of direct-access devices see figures 4a, 4b, and 4c.). Running time was 110 minutes for the first 12 hours and 90 minutes for each of the remaining 2 runs. This time could be reduced to a more operationally acceptable figure by changing from Fortran to machine language programming, conversion to one-dimensional arrays, and, in general, increased programming efficiency.

As originally planned, the 100-mb level was to have been completely inactive; that is, the equation

$$\nabla^2 \psi_t + \mathbf{V}_\psi \cdot \nabla \eta + \nabla \chi \cdot \nabla f = f \frac{\partial}{\partial p} (\omega + \Omega) \quad (36)$$

as applied at 100 mb is subject to the following boundary conditions:

$$\begin{aligned} \psi_t &= 0 \\ \mathbf{V}_\psi \cdot \nabla \eta &= 0 \\ \chi &= 0 \\ \omega + \Omega &= 0 \end{aligned}$$

In order to deduce improved values of vertical derivatives of the geopotential at 200 mb thus improving the static stability parameter, the heights at the 100-mb level were altered at each time step using the Navy regression procedure outlined in Appendix E. This procedure was intended to provide a reasonable estimate of the mean temperature in the 200 to 100-mb layer for use in the thermodynamic equation. Due to an inadvertent programming error, however, the Φ_{100} values were converted to a ψ_{100} field which varied in time. This lapse caused the alteration of the static boundary conditions above and, through the ω equation, it affected the values of $f \frac{\partial}{\partial p} J(\psi, \eta)$ in eq. (26), especially at the upper levels. The actual desired result of this term at 200 mb in centered finite-difference form is

$$\frac{f [J(\psi, \eta)_{300} - 0]}{200 \text{ mb}} \quad (37)$$

The effects on this important term of the ω -equation were operative from $t = 0$ but were not discernible until diverging values of ω were detected at $t = 42$ hours. It is planned to rectify this problem and report the results at a future date.

As is depicted in Table 2, the model appears to produce too much deepening at low levels and an overall increase in heights above 850 mb. The reason for this phenomenon is as yet undetermined. The fact that systems do indeed maintain their identity and that flow patterns, at least in a qualitative sense, show much similarity to the verifying analyses indicates that the model has some merit and further work on its refinement is justified.

TABLE 1

F(p) VALUES FOR USE IN EQUATION 14

(a) Gradient Level Assumed as 850 mb

Pressure level	F(p)
1000 mb	0.00000
850 mb	1.00000
700 mb	0.75178
500 mb	0.42534
300 mb	0.13528
200 mb	0.03398
100 mb	0.00000

(b) Gradient Level Assumed as 700 mb

Pressure level	F(p)
1000 mb	0.00000
850 mb	0.20763
700 mb	1.00000
500 mb	0.56579
300 mb	0.17995
200 mb	0.04520
100 mb	0.00000

TABLE 2

ROOT MEAN SQUARE ERROR RESULTS

	12 HR. FCST. RMSE	PILLOW	24 HR. FCST. RMSE	PILLOW	36 HR. FCST. RMSE	PILLOW
1000 mb	31.8	-11.2	50.1	-13.7	69.7	-13.7
850 mb	26.4	- 0.5	43.9	- 0.2	60.5	- 0.0
700 mb	26.5	9.3	44.4	14.1	60.7	14.2
500 mb	39.5	29.8	60.3	37.5	79.4	35.6
300 mb	64.8	65.1	86.9	77.0	109.2	75.2
200 mb	78.9	83.8	97.0	95.9	116.9	93.4

Values in Meters

Level Diagram

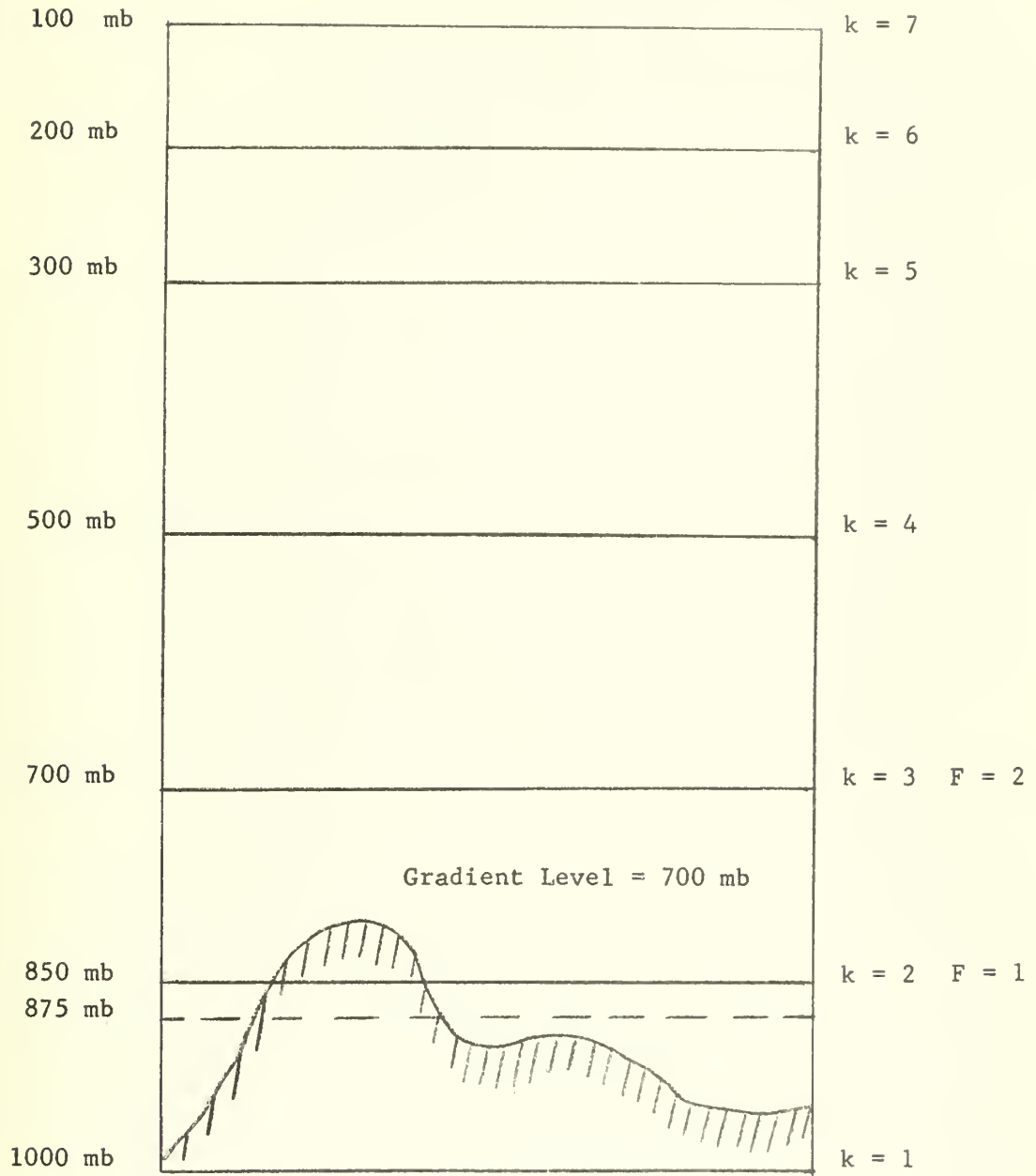


Figure 1

Schematic representation of the pressure surfaces used in the diagnostic procedures. The index $k = 1, \dots, 7$ is identified with the constant pressure values shown in mb. The index $F = 1, 2$ denotes the top of the atmospheric boundary level or gradient level, of 850 mb, or 700 mb, the selection of which depends upon the station pressure $p_T(i, j)$.

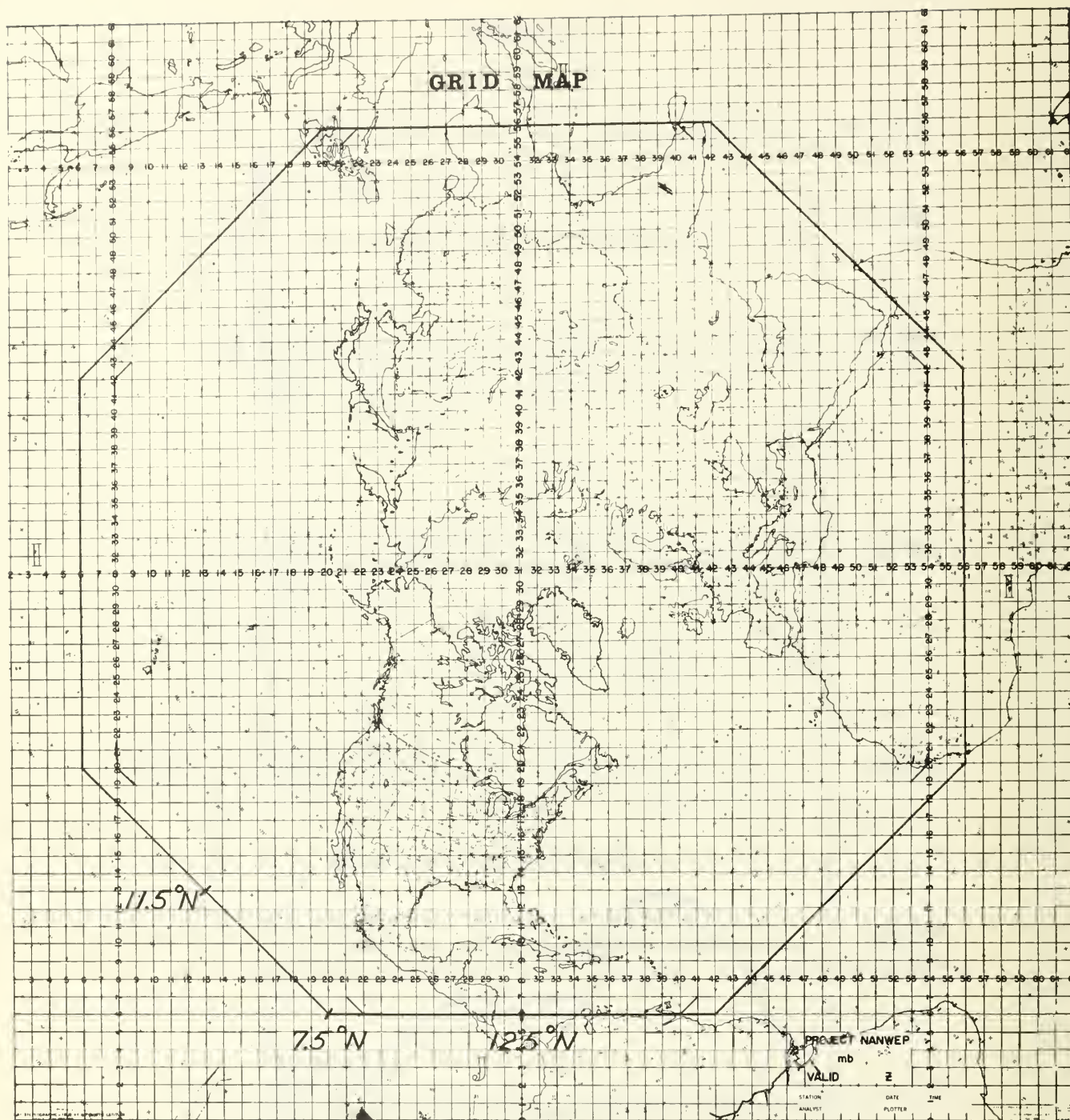


Figure 2

FLOW DIAGRAM

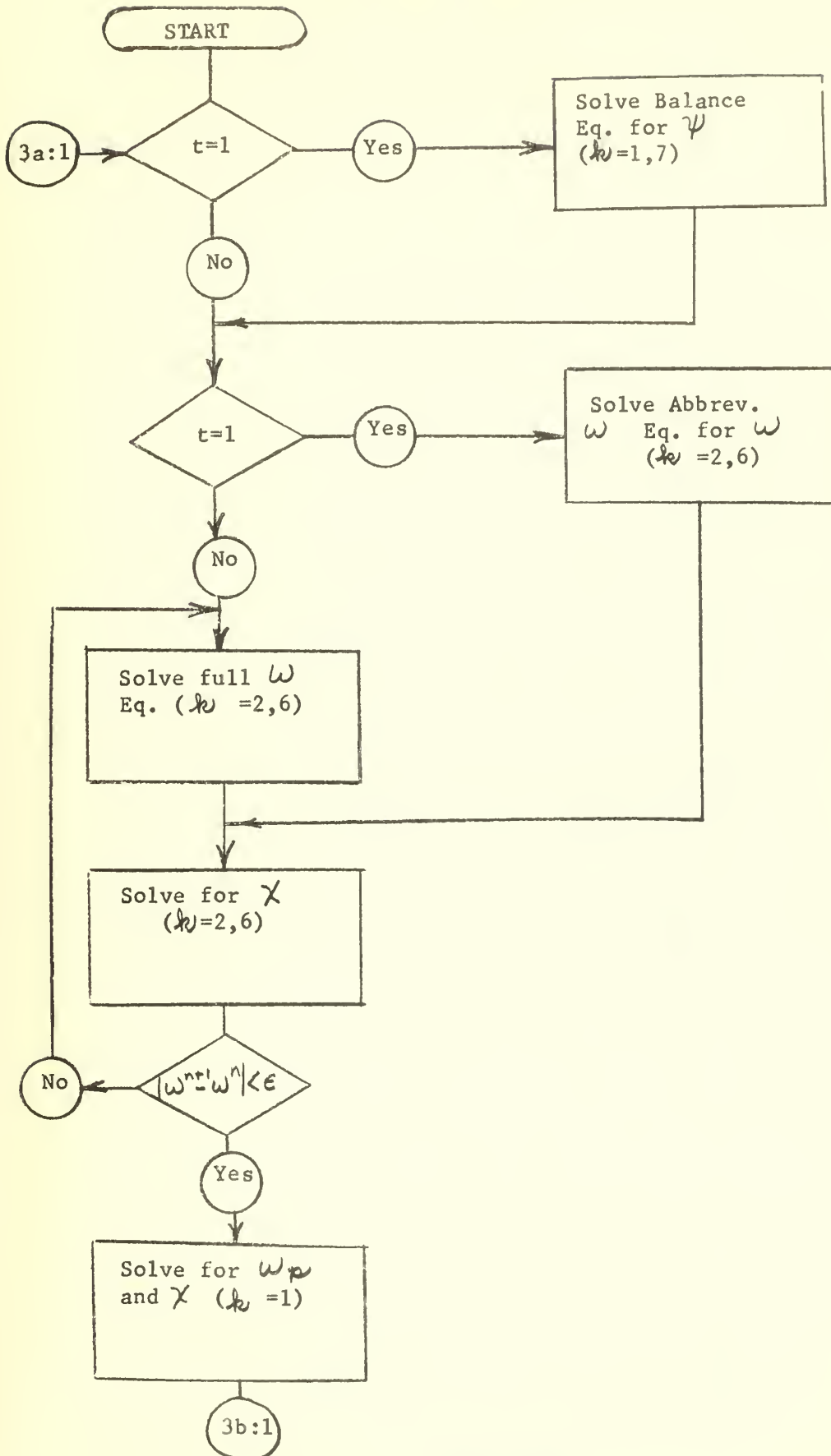


Figure 3a.

FLOW DIAGRAM (continued)

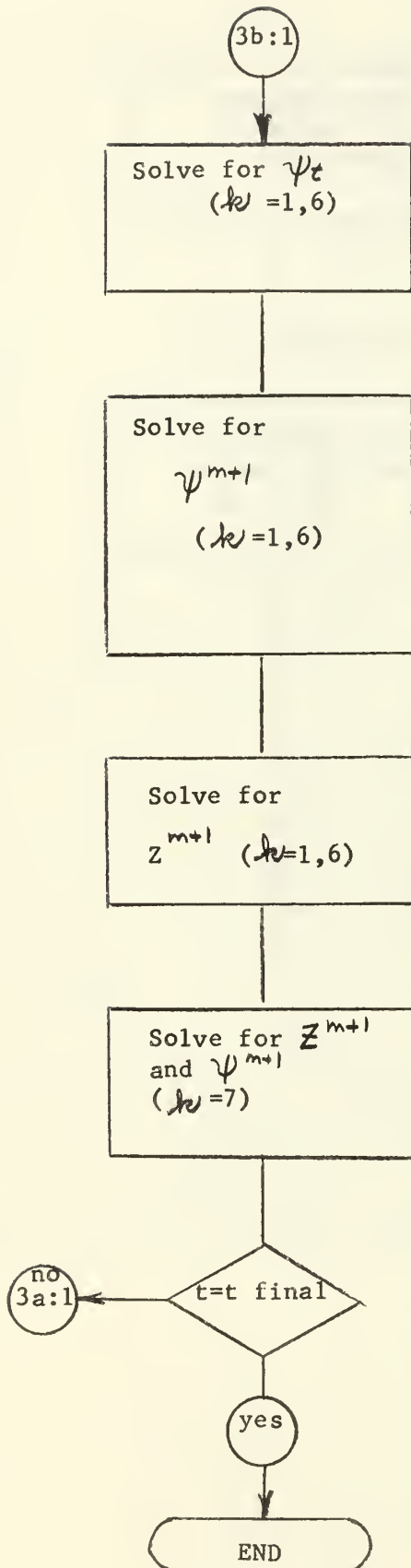


Figure 3b

TAPE 11 RECORD LAYOUT

Record	Contents
1.	1000-mb initial Z values
2.	850-mb initial Z values
3.	700-mb initial Z values
4.	500-mb initial Z values
5.	300-mb initial Z values
6.	200-mb initial Z values
7.	100-mb initial Z values
8.	Z_o -values
9.	Z_T -values

Figure 4a

DISK 12 AND 13 RECORD LAYOUT

Record	Contents
1.	1000-mb Z intermediate forecast
2.	1000-mb ψ previous time intermediate forecast
3.	1000-mb ψ current time intermediate forecast
4.	1000-mb ω intermediate forecast
5.	1000-mb χ intermediate forecast
6-10.	contents & sequence same as Records 1-5 for 850 mb
11-15.	contents & sequence same as Records 1-5 for 700 mb
16-20.	contents & sequence same as Records 1-5 for 500 mb
21-25.	contents & sequence same as Records 1-5 for 300 mb
26-30.	contents & sequence same as Records 1-5 for 200 mb
31-35.	contents & sequence same as Records 1-5 for 100 mb

Figure 4b

TAPE 14 RECORD LAYOUT

Record	Contents
1.	1000-mb Z final forecast ³
2.	1000-mb ψ previous time final forecast
3.	1000-mb ψ current time final forecast
4.	1000-mb ω final forecast
5.	1000-mb χ final forecast
6-10.	Contents & sequence same as Records 1-5 for 850 mb
11-15.	Contents & sequence same as Records 1-5 for 700 mb
16-20.	Contents & sequence same as Records 1-5 for 500 mb
21-25.	Contents & sequence same as Records 1-5 for 300 mb
26-30.	Contents & sequence same as Records 1-5 for 200 mb
31-35.	Contents & sequence same as Records 1-5 for 100 mb
36-70.	Contents & sequence same as Records 1-35 for 2nd forecast interval

Figure 4c

³Note: Although these records are designated as final forecast, they are used as input for the next computer interval run if the total forecast is partitioned into forecast interval segments.

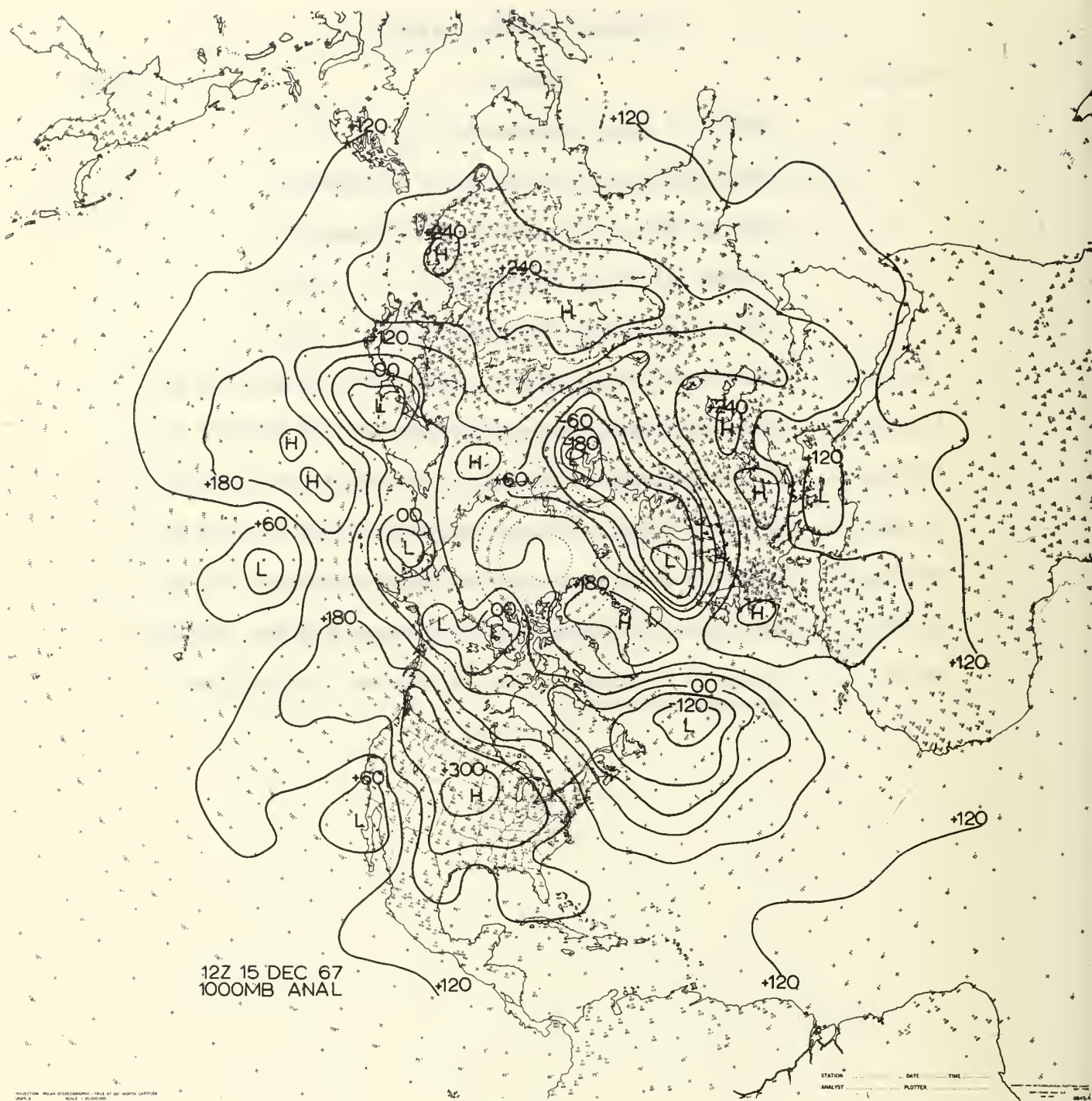


Figure 5

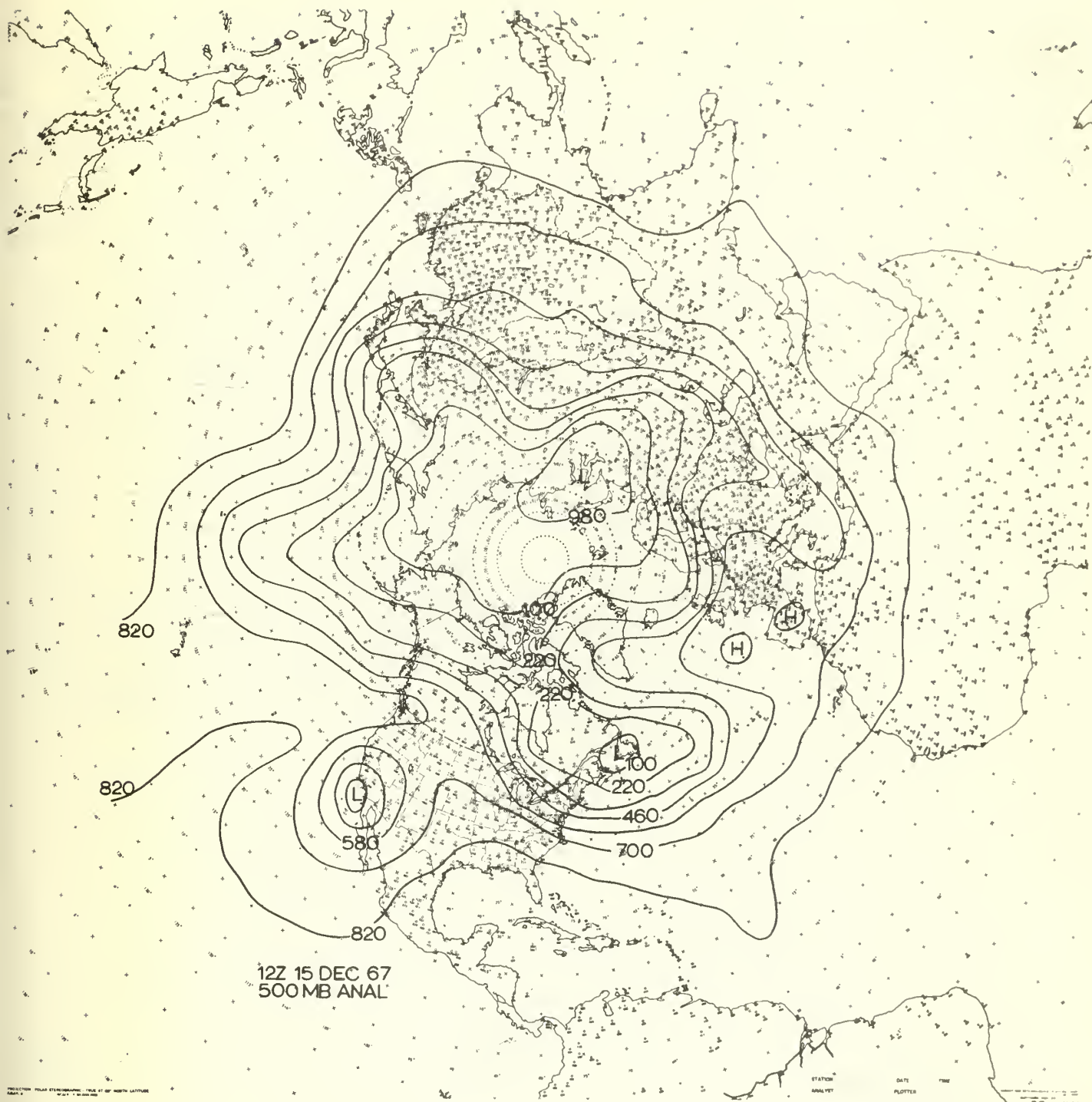


Figure 6

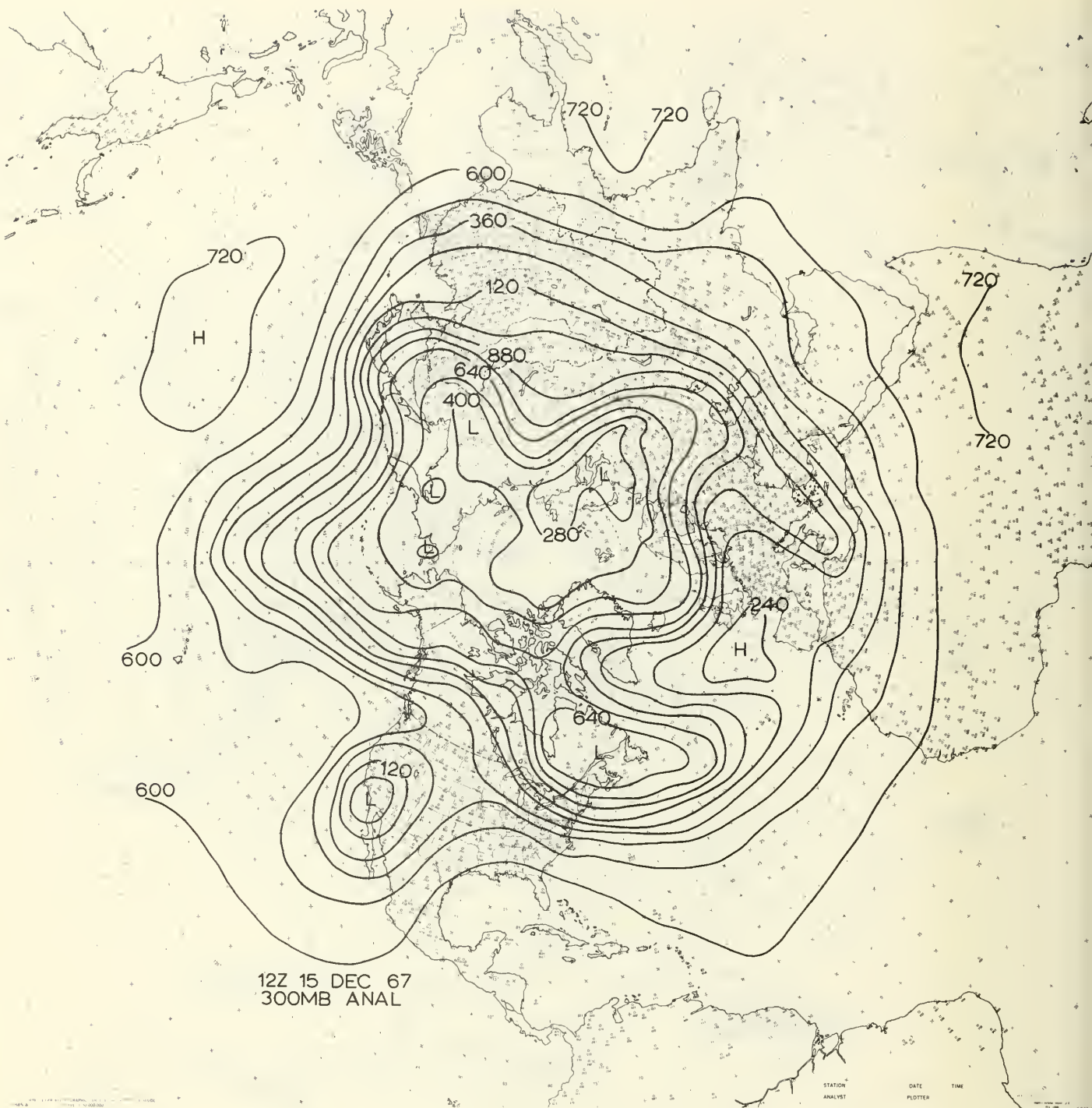


Figure 7



Figure 8

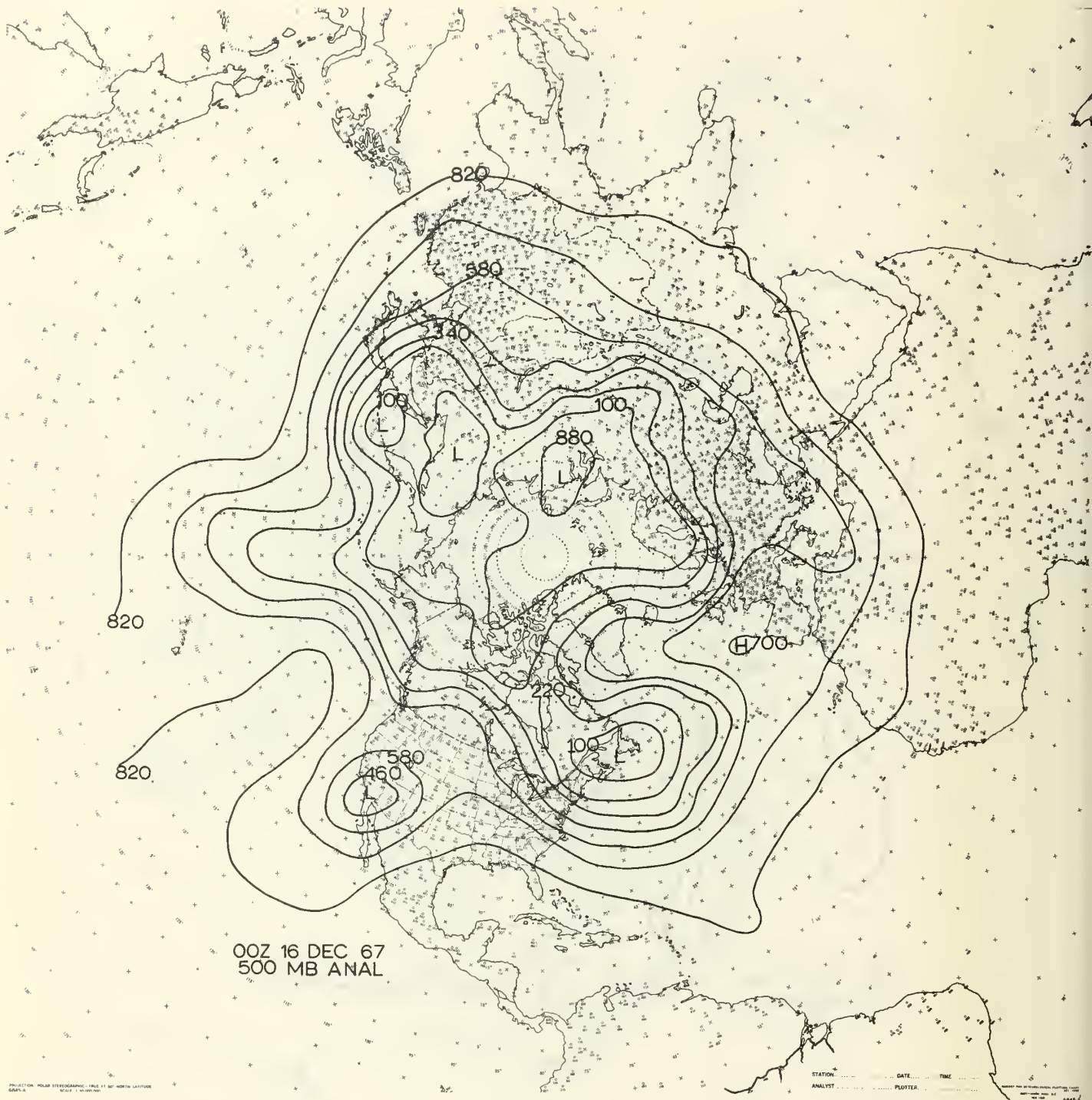


Figure 9

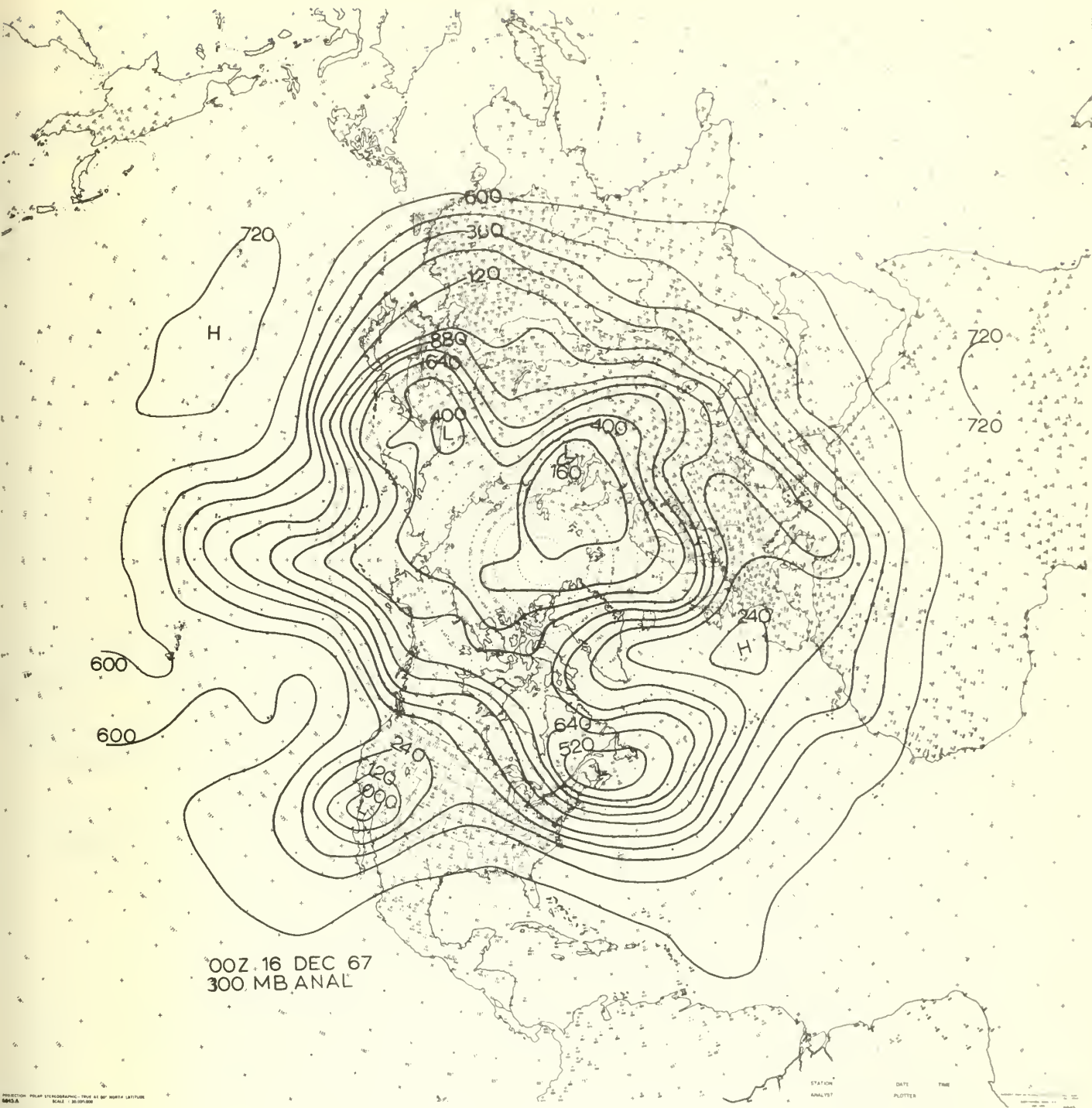


Figure 10

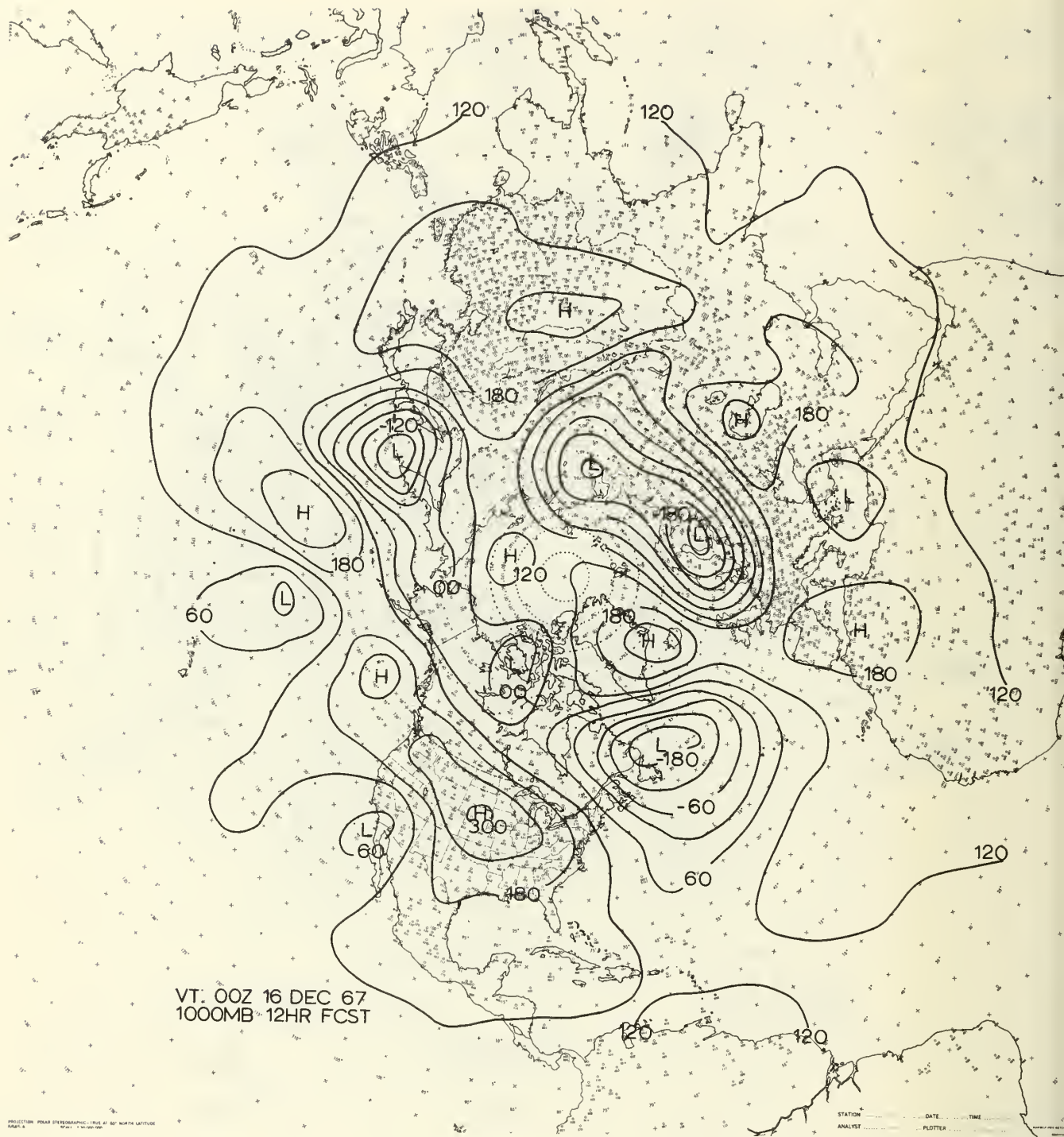


Figure 11

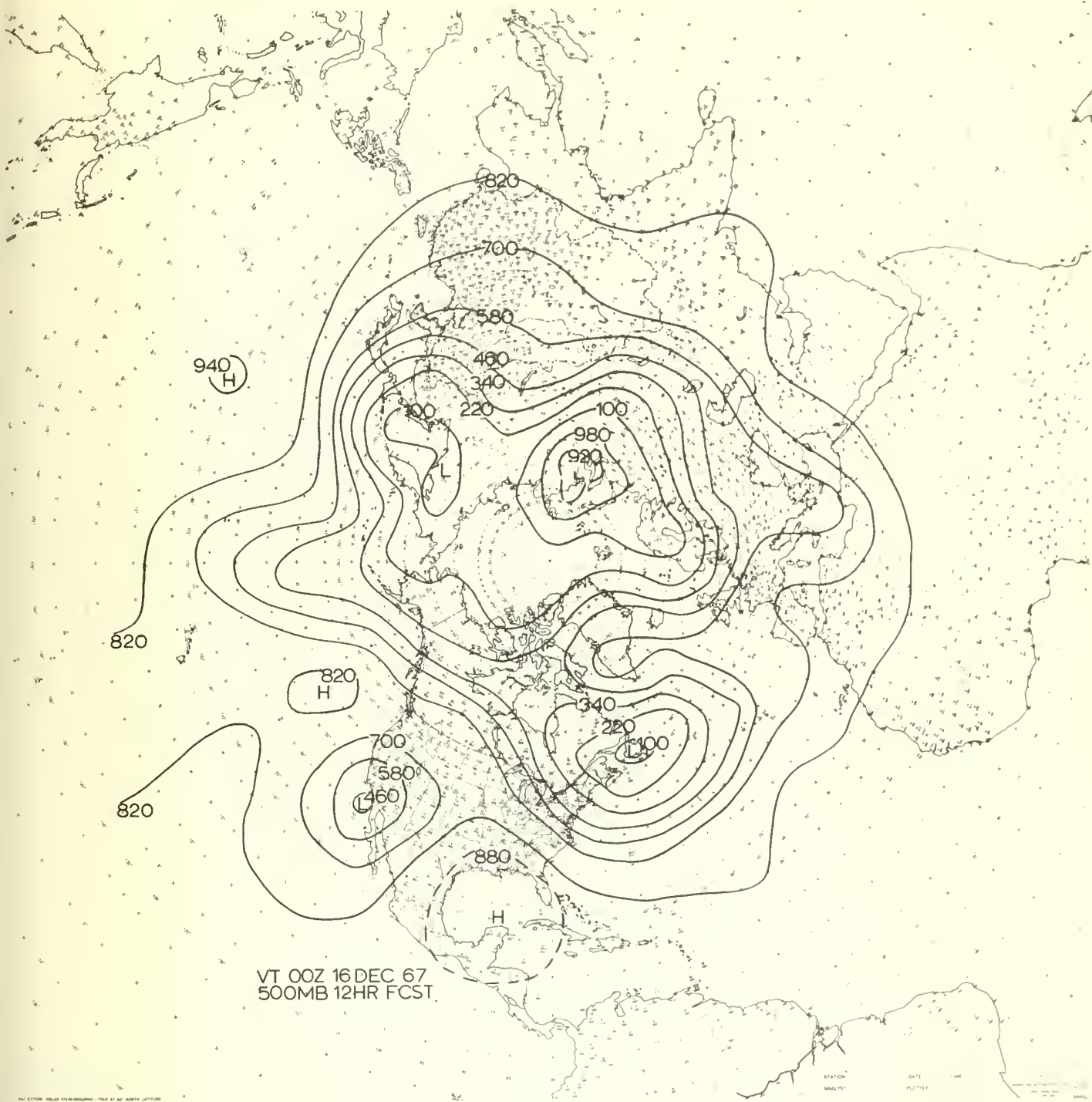


Figure 12

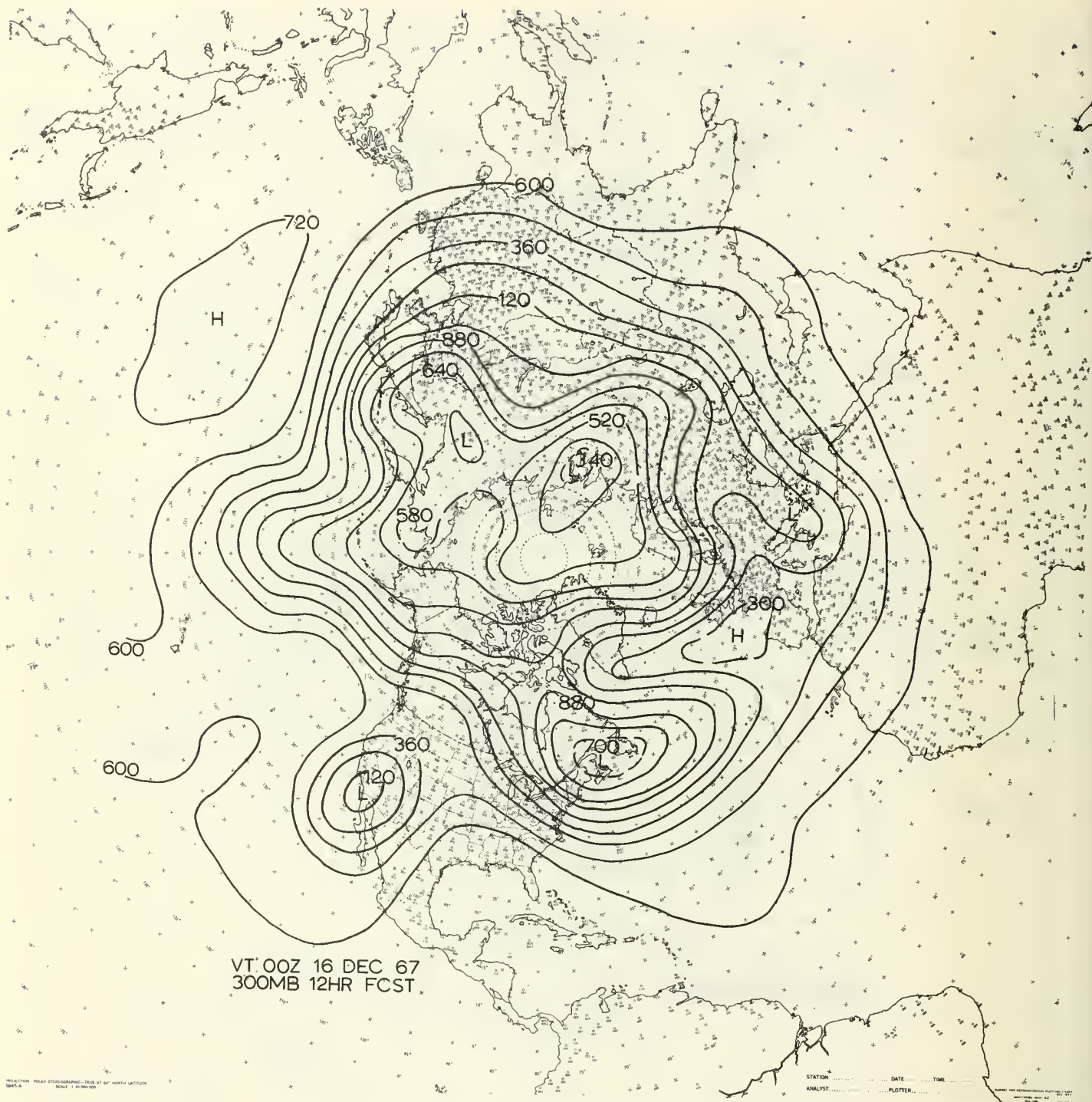


Figure 13

0

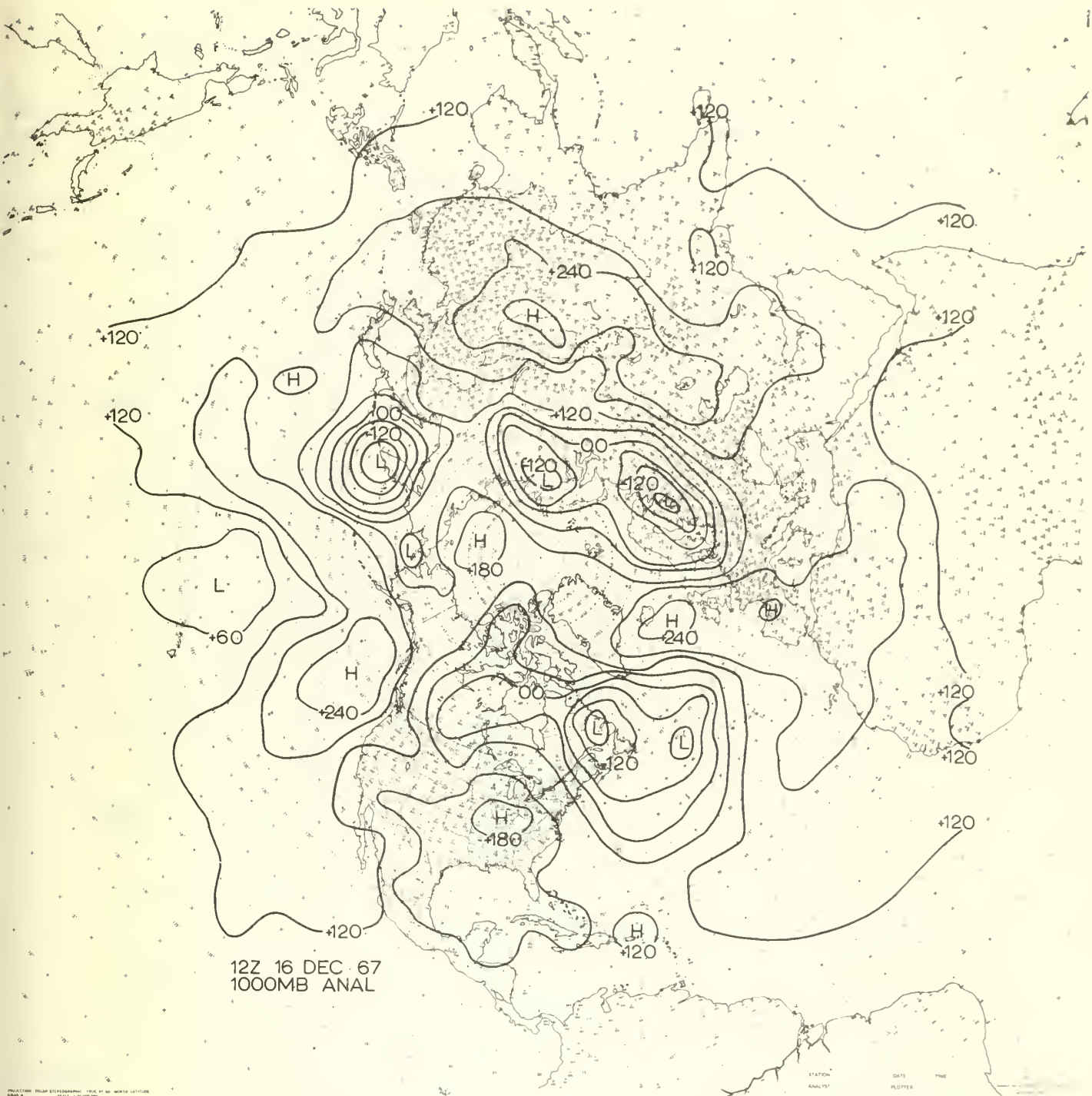


Figure 14

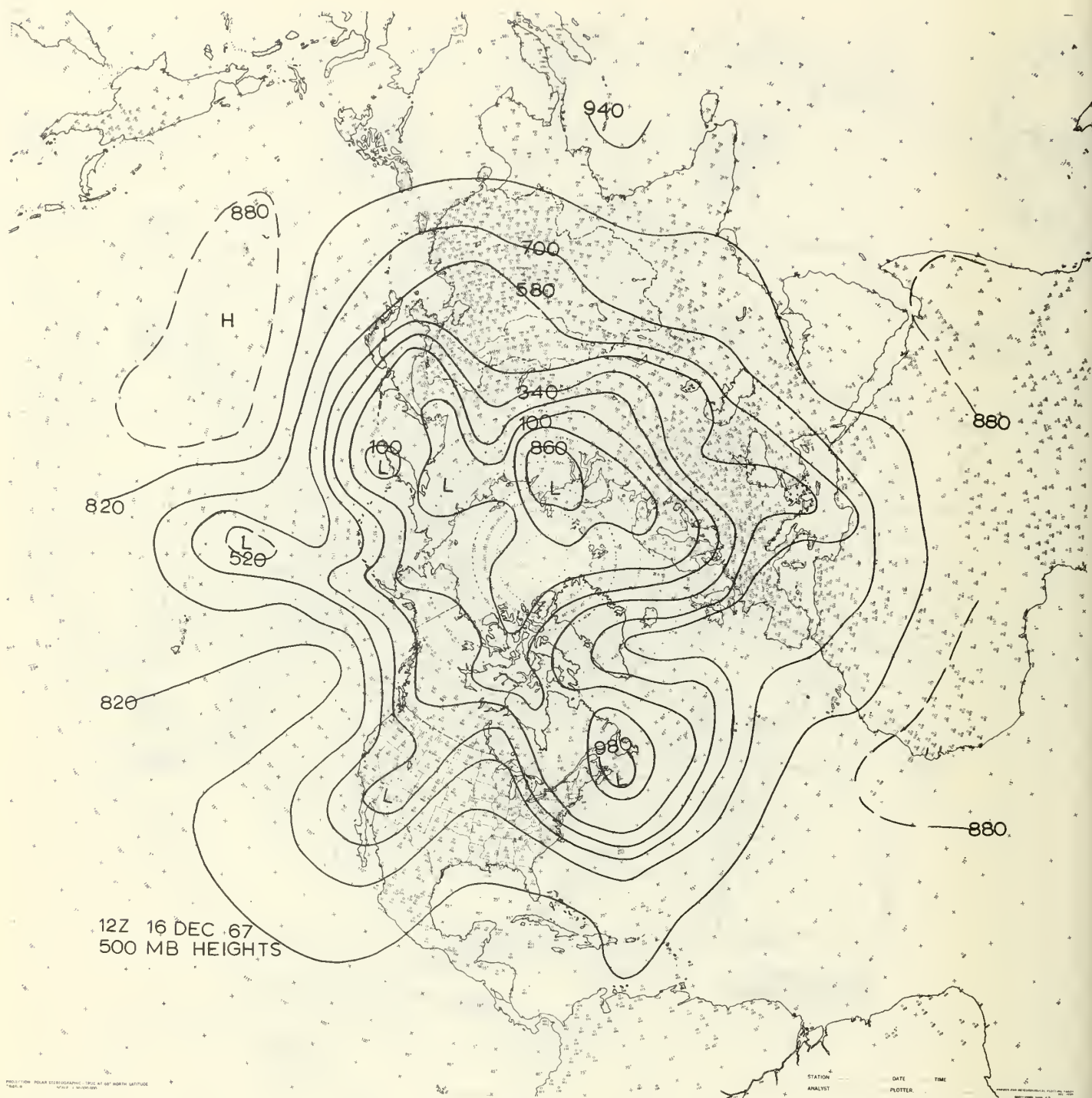


Figure 15

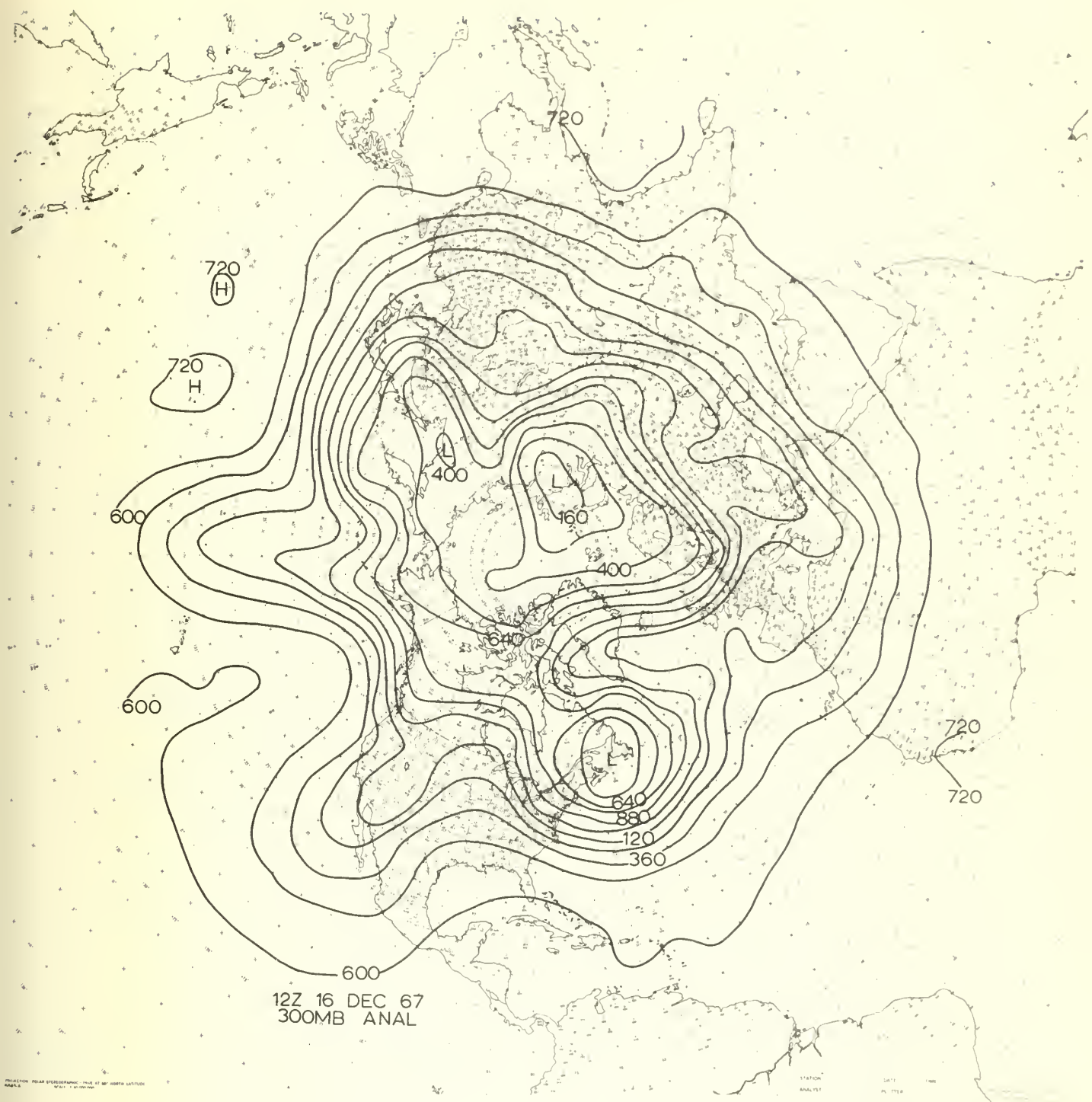


Figure 16

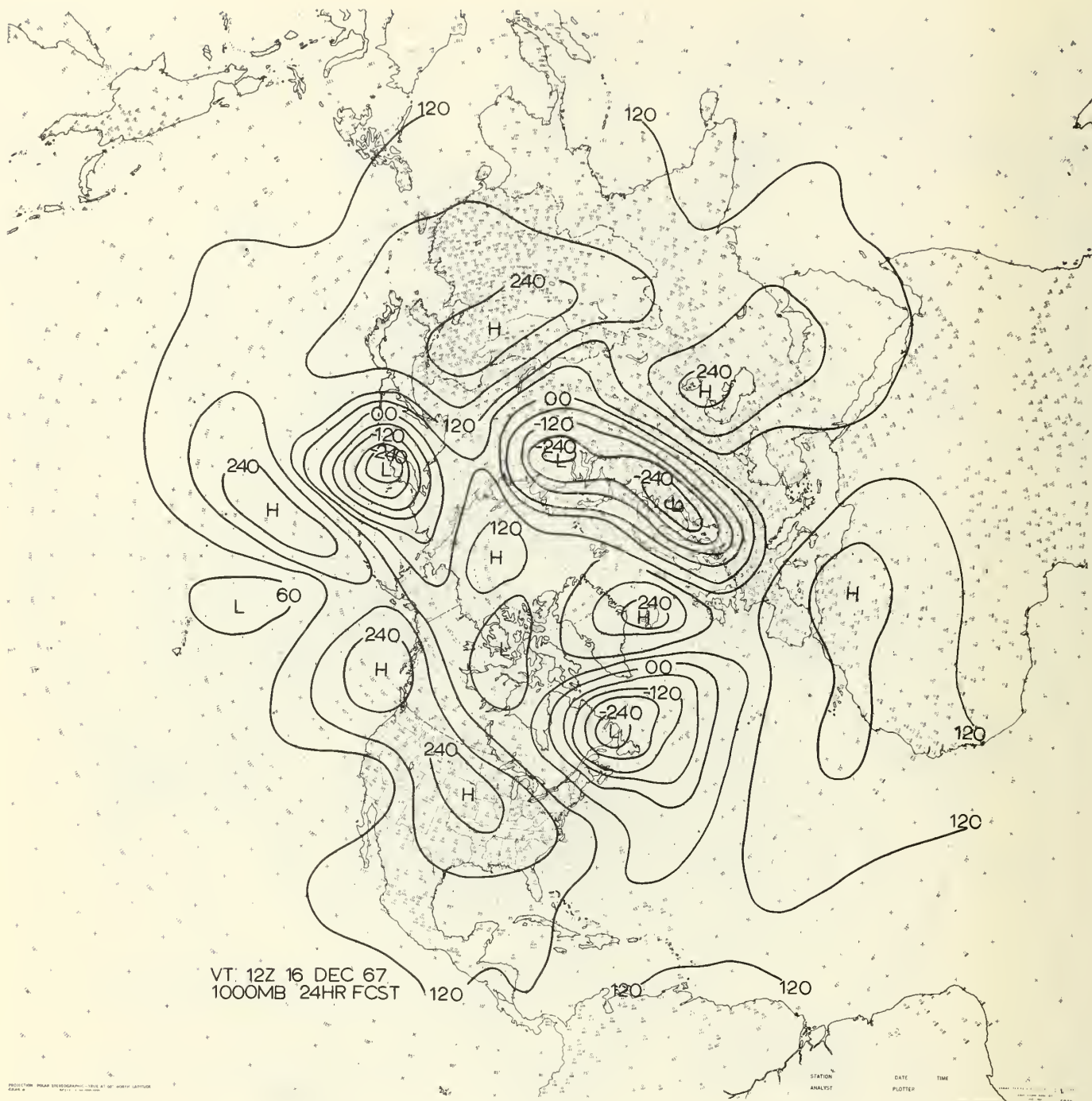


Figure 17

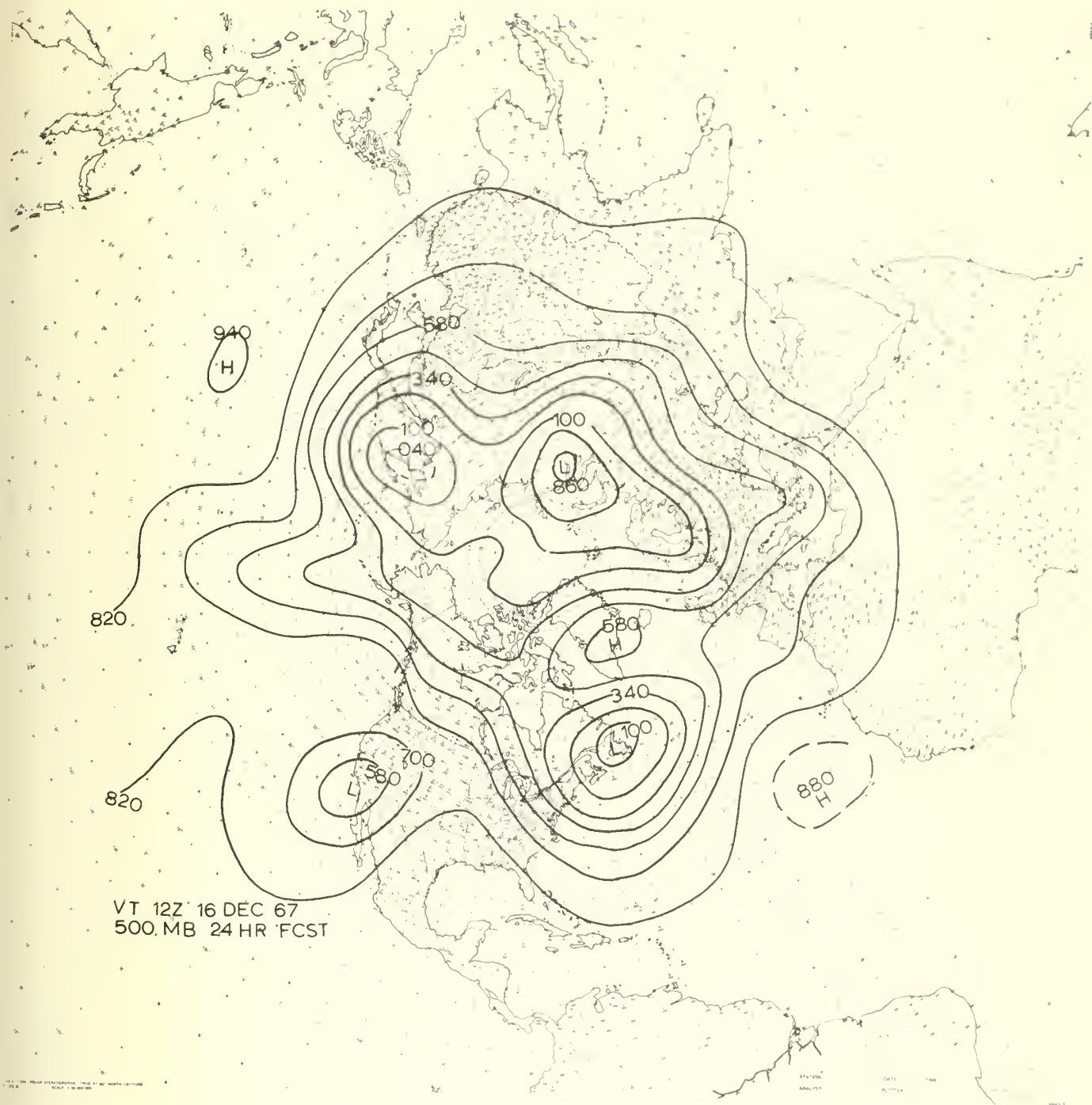


Figure 18

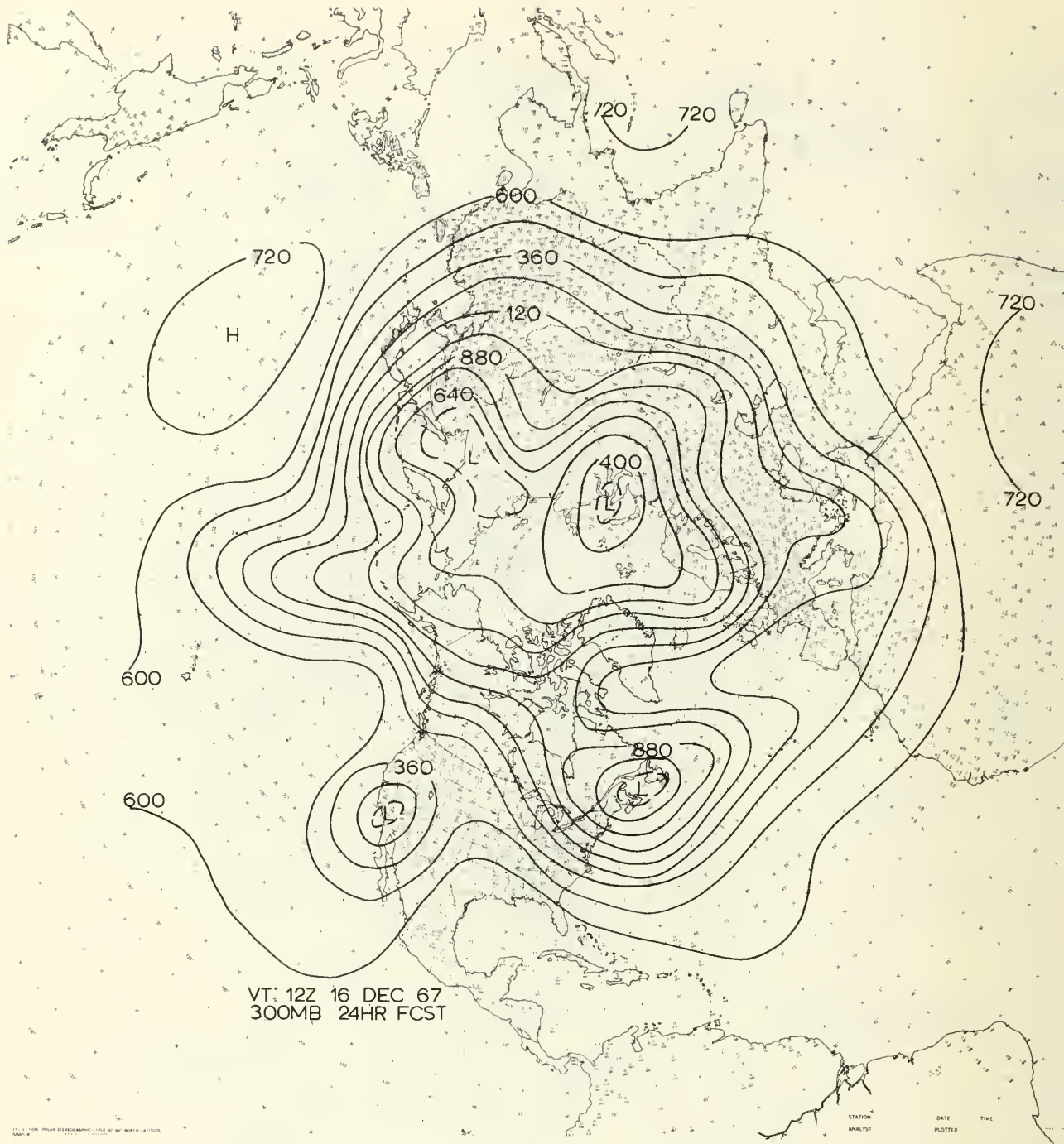


Figure 19

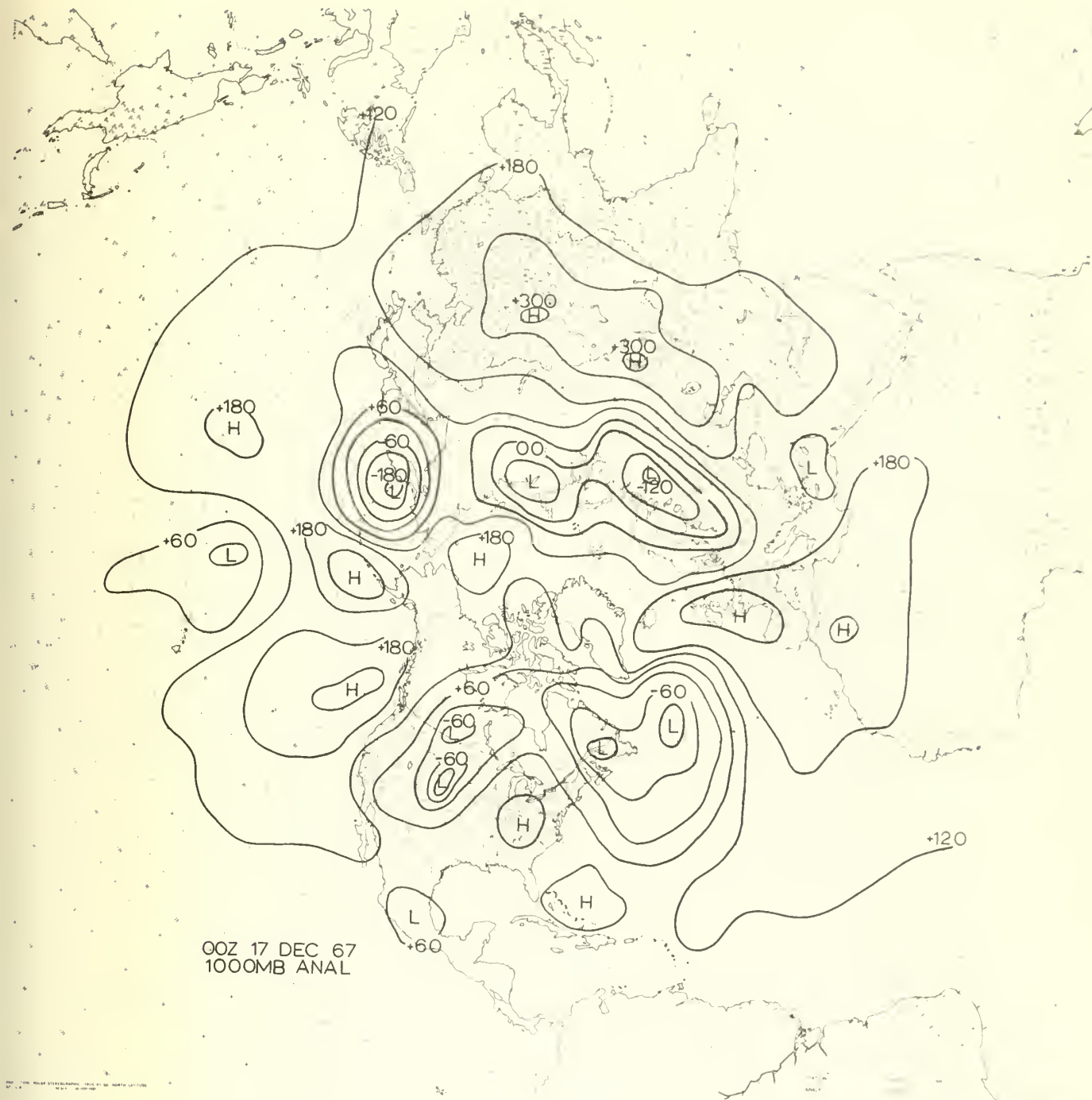


Figure 20

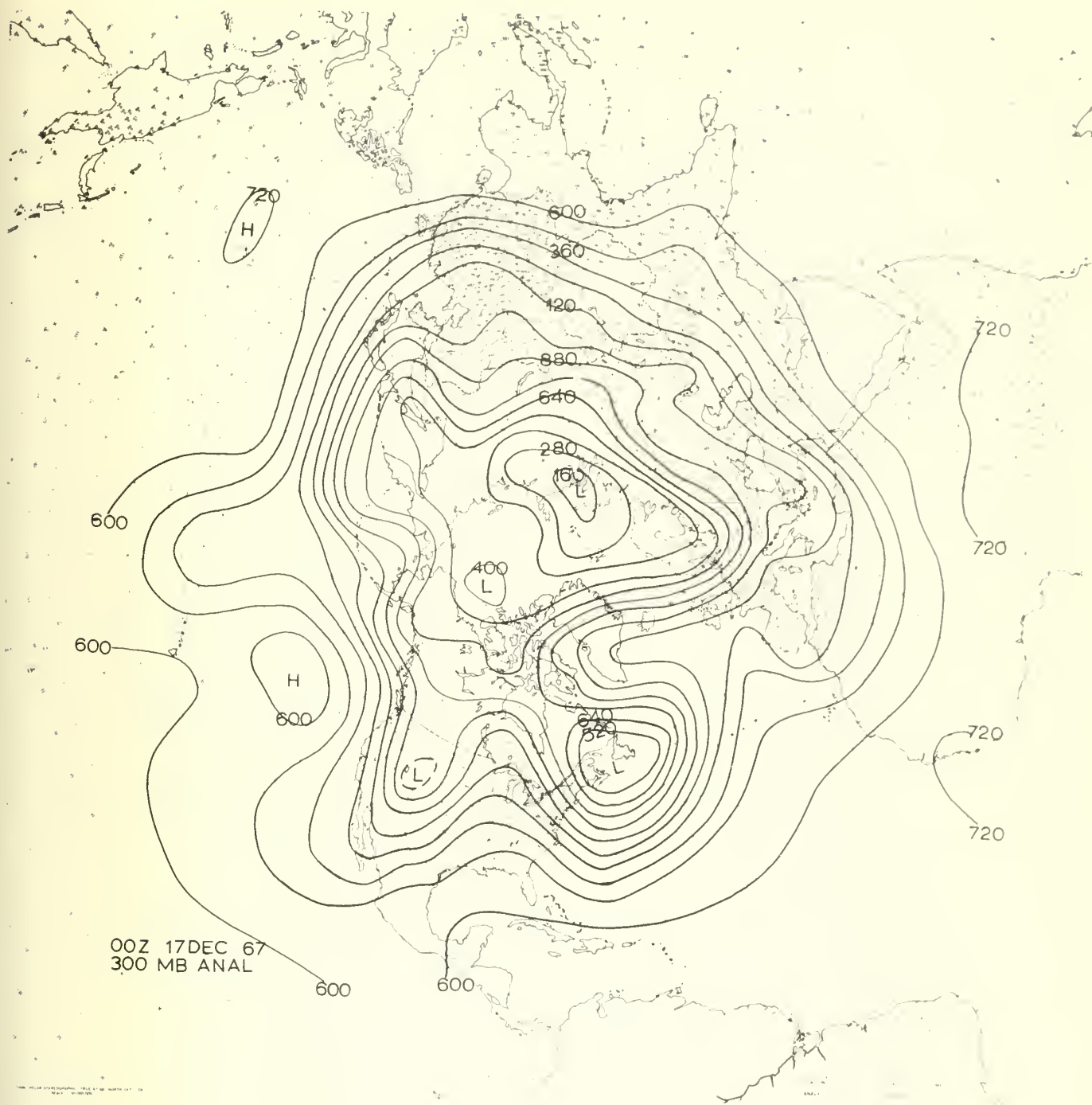


Figure 22

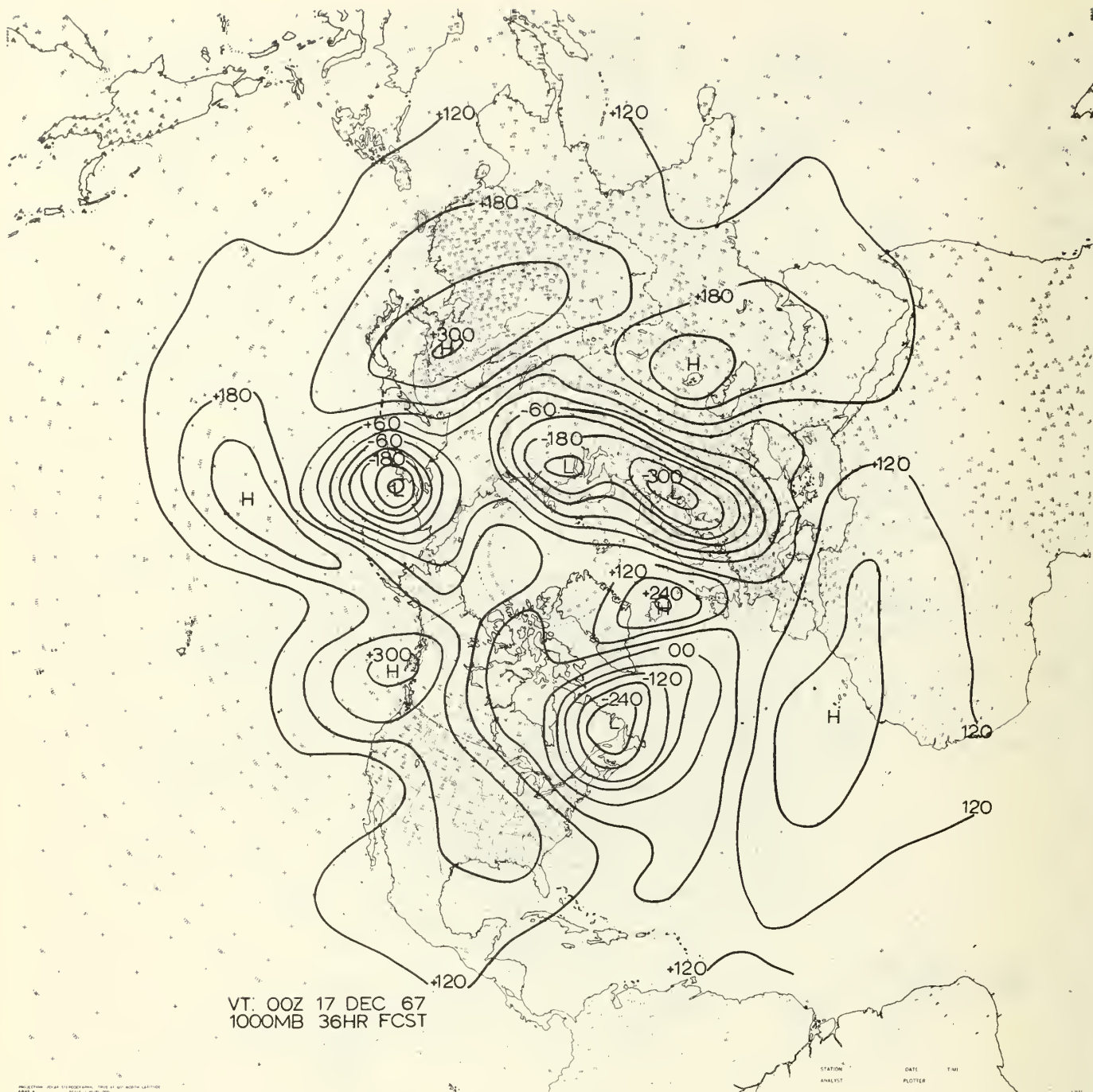


Figure 23

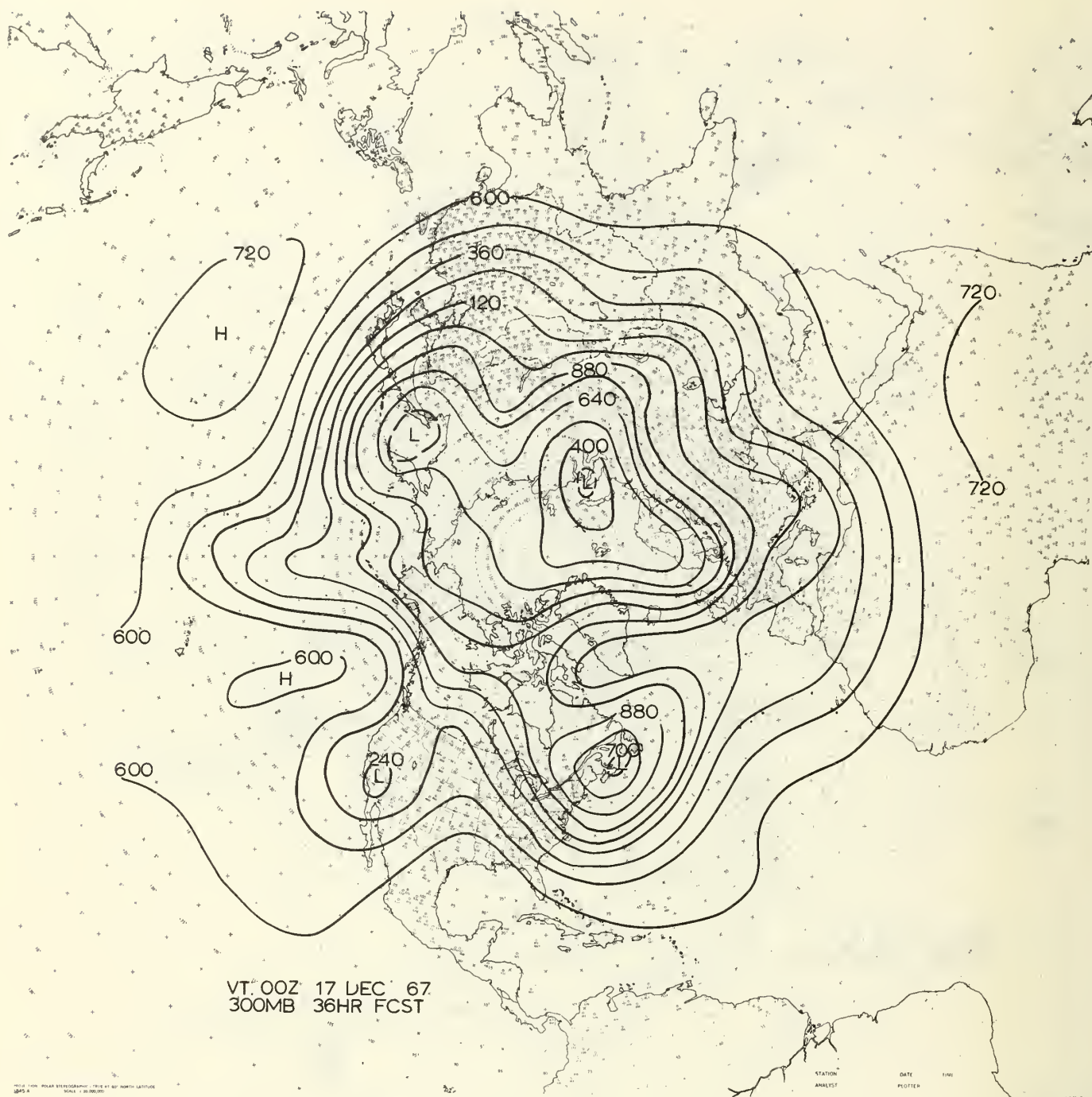


Figure 25

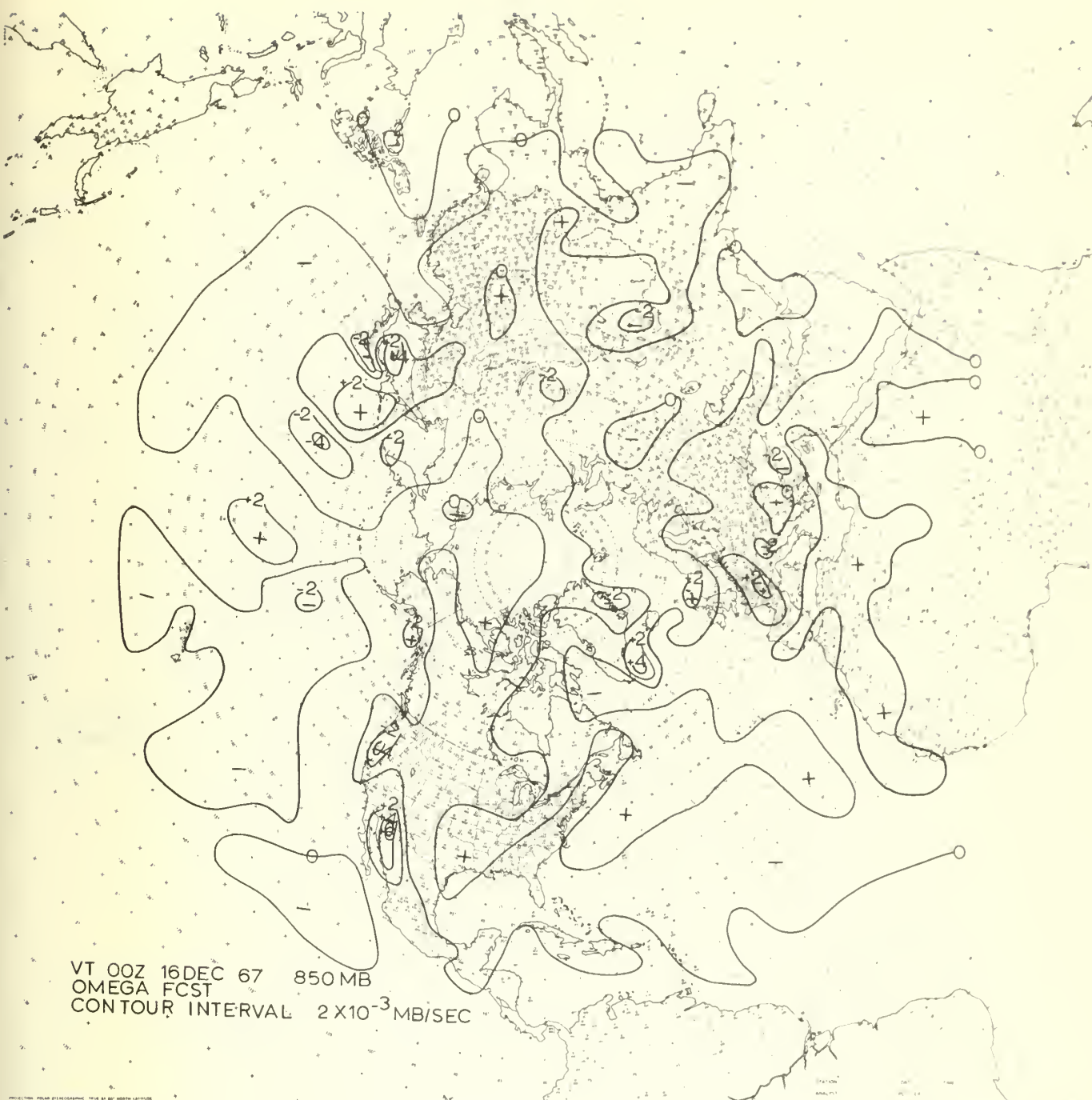


Figure 26

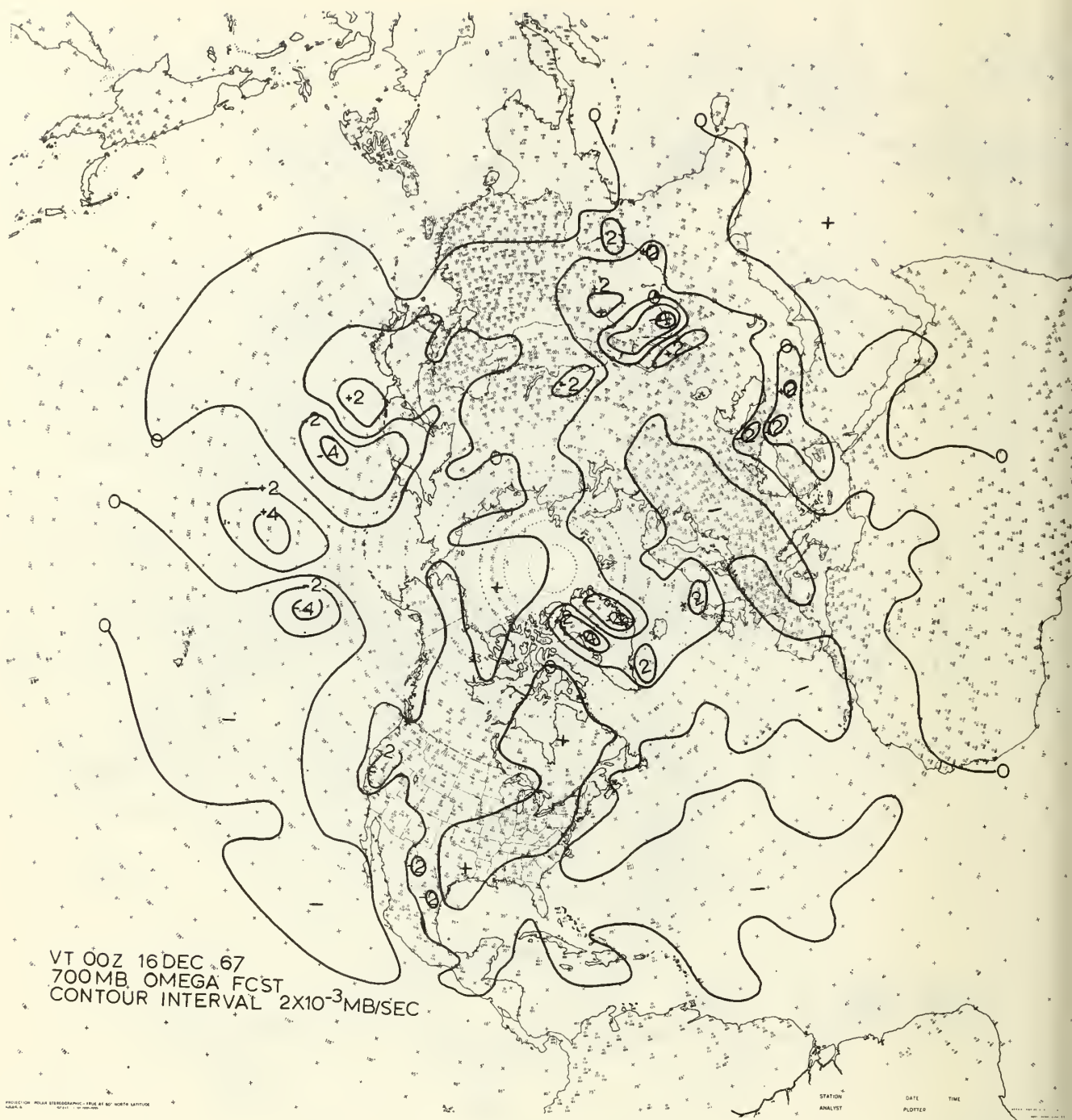


Figure 27

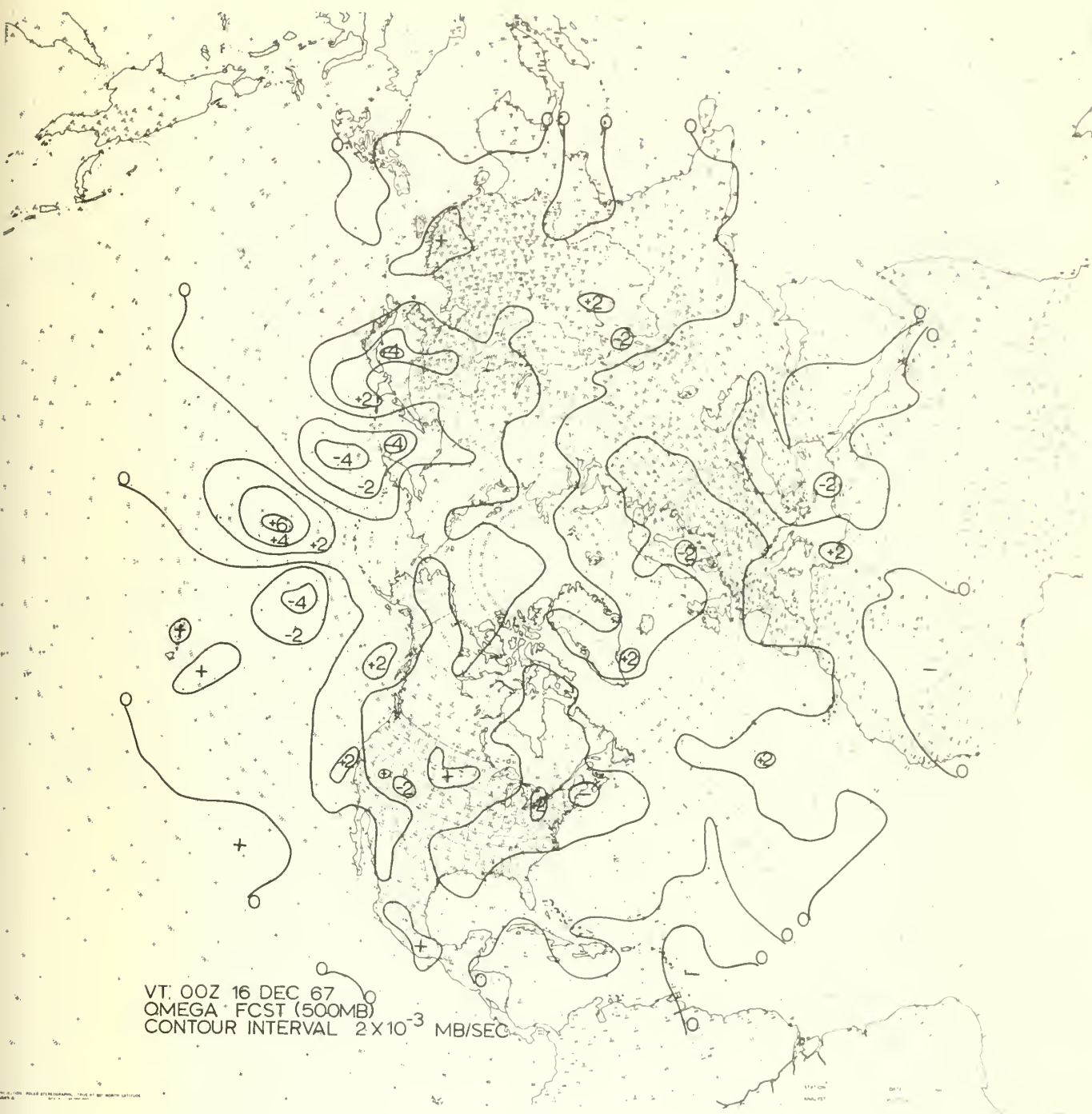


Figure 28

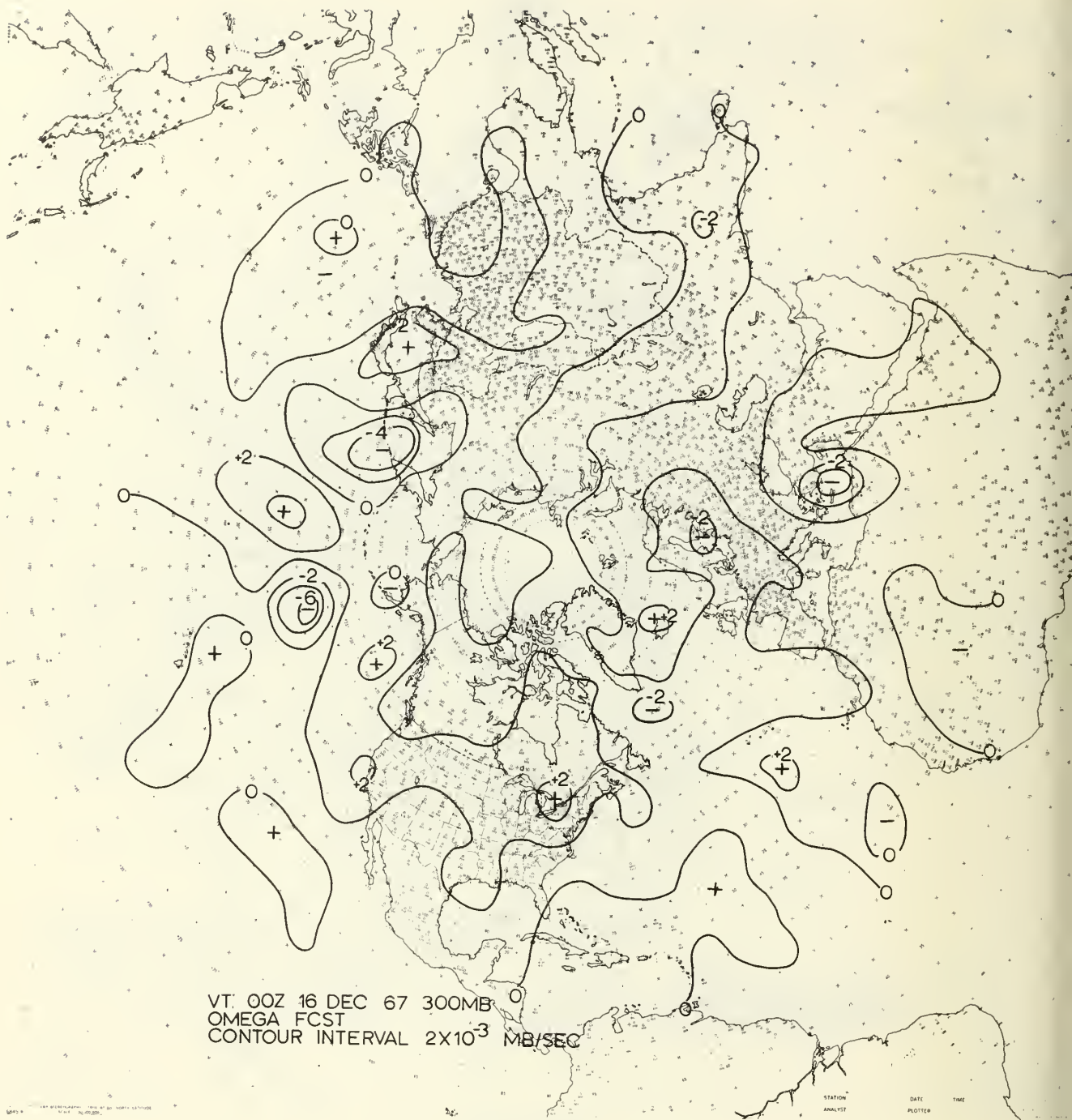


Figure 29



Figure 30

BIBLIOGRAPHY

1. Arakawa, A., 1962: Non-geostrophic Effects in the Baroclinic Prognostic Equations. Proceedings of the International Weather Prediction Symposium in Tokyo, Nov. 7-13, 1960, Meteorological Society of Japan, pp. 161-175.
2. Berkofsky, L. and E. A. Bertoni, 1955: Mean Topographical Charts of the Entire Earth. Bulletin of the American Meteorological Society, Vol. 36, pp. 350-354.
3. Cressman, G. P., 1960: Improved Terrain Effects in Barotropic Forecasts. Monthly Weather Review, Vol. 88, pp. 327-342.
4. Danard, Maurice B., 1966: A Quasi Geostrophic Numerical Model Incorporating Effects of Release of Latent Heat. Journal of Applied Meteorology, Vol. 5, pp. 85-93.
5. Estoque, M., 1957: A Graphically Integrable Prediction Model Incorporating Orographic Influences. Journal of Applied Meteorology, Vol. 14, pp. 293-296.
6. Graham, Ian K., 1968: Calculations of Surface Stress. B. S. Paper, Department of Meteorology and Oceanography, Naval Post-Graduate School.
7. Grimmering, G., 1941: The Intensity of Lateral Mixing in the Atmosphere as Determined from Isentropic Charts. Bulletin of the American Meteorological Society, Vol. 22, pp. 227-233.
8. Haltiner, G. J., L. C. Clarke and G. E. Lawniczak, Jr., 1963: Computation of the Large Scale Vertical Velocity, Journal of Applied Meteorology, Vol. 2, pp. 242-249.
9. Haltiner, G. J. and F. L. Martin, 1957: Dynamical and Physical Meteorology, McGraw-Hill Book Co., Inc., New York, p. 55.
10. Jennings, W., 1964: First Course in Numerical Methods, Macmillan Company, New York, p. 79.
11. Krishnamurti, T. N., 1968: A Study of a Developing Wave Cyclone. Monthly Weather Review, Vol. 96, pp. 208-217.
12. Kung, E. C., 1963: Climatology of Aerodynamic Roughness Parameter and Energy Dissipation in the Planetary Boundary Layer of the Northern Hemisphere. Studies of the Effects of Variations in Boundary Conditions on the Atmospheric Boundary Layer, University of Wisconsin, Madison, Wisconsin, pp. 37-96.

13. Lea, Duane A., 1961: Regression Equations for Vertical Extrapolation of Constant Pressure Surface Heights and Temperatures between 200 mb and 30 mb. 191st Meeting of the AMS, Chicago, Illinois, March 1961.
14. Richtmyer, R. D. and K. W. Morton, 1967: Difference Methods for Initial Value Problems, Interscience Publishers, New York, pp. 189-192.
15. Shuman, Frederick G., and John B. Hovermale, 1967: An Operational Six-Layer Primitive Equation Model, National Meteorological Center, Weather Bureau, ESSA, Washington, D. C. 59 pp.
16. Thompson, P. D., 1961: Numerical Weather Analysis and Prediction, Macmillan Co., New York, 70 pp.
17. United States Committee on Extension to the Standard Atmosphere, 1962: U. S. Standard Atmosphere, 1962, U. S. Government Printing Office, Washington, D. C., 278 pp.

APPENDIX A

Computation of Terrain Pressure

In exhibiting the method of determination of terrain pressure p_T the example used will be the case of terrain lower than the 850-mb standard height. Here Z_T is the terrain height, Z_1 is the 1000-mb height and Z_2 is the 850-mb height. We start with the hypsometric relationship:

$$Z_T - Z_1 = \frac{R_d}{g} \bar{T} \ln \frac{p_1}{p_T} \quad (A-1)$$

In (A-1), \bar{T} is the mean temperature in the layer. Equation A-1 may also be expressed as

$$\Delta Z = \Delta Z_{ST} [1 + \bar{S}_v] \quad (A-2)$$

where \bar{S}_v is the mean specific virtual temperature anomaly as discussed in Haltiner and Martin (1957) and subscript ST refers to standard atmosphere value. After replacing temperature,

$$\bar{T} = -\frac{1}{R_d} \frac{\partial \Phi}{\partial \ln p}$$

the following approximation for $1 + \bar{S}_v$ is obtained in finite-difference form:

$$1 + \bar{S}_v = \frac{\Phi_2 - \Phi_1}{(\Phi_2 - \Phi_1)_{ST}} = \frac{\Delta Z}{\Delta Z_{ST}} \quad (A-3)$$

Since ΔZ is known at any time, $\Delta Z_{ST} = (Z_T - Z_1)_{ST}$ may be determined by the substitution of (A-3) into (A-2); hence, a value of $(Z_T)_{ST}$ may be obtained. This value is compared with standard atmosphere heights from U. S. Standard Atmosphere (1962). When the height values are matched, the corrected terrain pressure is determined.

For cases in which the terrain extends above the 850-mb standard height, the same procedure is followed and sub 1 refers to 850 mb and sub 2 refers to 700 mb, and similarly for higher terrain heights.

APPENDIX B

Treatment of Vertical Derivatives

For fitting ω (vertical motion) profiles to three successive pressure levels (lower level subscript 1, middle level subscript 2, upper level subscript 3) a Lagrangian quadratic interpolation formula is used on omega.

$$\omega(p) = \omega_1 \frac{(p-p_2)(p-p_3)}{(p_1-p_2)(p_1-p_3)} + \omega_2 \frac{(p-p_1)(p-p_3)}{(p_2-p_1)(p_2-p_3)} + \omega_3 \frac{(p-p_1)(p-p_2)}{(p_3-p_1)(p_3-p_2)} \quad (B-1)$$

After differentiating the above and setting $p = p_2$ the following equation is obtained:

$$\left. \frac{\partial \omega}{\partial p} \right)_{p=p_2} = \omega_1 \frac{(p_2-p_3)}{(p_1-p_2)(p_1-p_3)} + \omega_2 \frac{(p_1-2p_2+p_3)}{(p_1-p_2)(p_2-p_3)} + \omega_3 \frac{(p_2-p_1)}{(p_3-p_1)(p_3-p_2)} \quad (B-2)$$

Similarly, differentiating (B-1) twice with respect to pressure and setting $p = p_2$ the following equation is obtained:

$$\left. \frac{\partial^2 \omega}{\partial p^2} \right)_{p=p_2} = 2 \left[\frac{\omega_1}{(p_1-p_2)(p_1-p_3)} + \frac{\omega_2}{(p_2-p_1)(p_2-p_3)} + \frac{\omega_3}{(p_3-p_1)(p_3-p_2)} \right] \quad (B-3)$$

Ω , the frictional and terrain induced vertical motion, is treated the same as ω in relation to the format of vertical derivatives.

For fitting Φ (geopotential) and ψ (streamfunction) to three successive pressure levels the same procedure, as above is followed with the exception that Φ and ψ are considered to have a quadratic vertical variation on a logarithmic pressure scale leading to the following results for Φ centered at $p = p_2$.

$$\Phi(p) = \Phi_1 \frac{(P-P_2)(P-P_3)}{(P_1-P_2)(P_1-P_3)} + \Phi_2 \frac{(P-P_1)(P-P_3)}{(P_2-P_1)(P_2-P_3)} + \Phi_3 \frac{(P-P_1)(P-P_2)}{(P_3-P_1)(P_3-P_2)} \quad (B-4)$$

where $P = \ln(p)$ and

$$\left. \frac{\partial \Phi}{\partial p} \right|_{p=P_2} = \frac{1}{p} \left[\frac{\Phi_1 \ln\left(\frac{P_2}{P_3}\right)}{\ln\left(\frac{P_1}{P_2}\right) \ln\left(\frac{P_1}{P_3}\right)} + \frac{\Phi_2 \ln\left(\frac{P_1 P_3}{P_2^2}\right)}{\ln\left(\frac{P_1}{P_2}\right) \ln\left(\frac{P_2}{P_3}\right)} + \frac{\Phi_3 \ln\left(\frac{P_2}{P_1}\right)}{\ln\left(\frac{P_2}{P_3}\right) \ln\left(\frac{P_1}{P_3}\right)} \right] \quad (B-5)$$

For $\frac{\partial \omega}{\partial p}$ at the 1000-mb level, omega is expressed as a cubic equation in terms of omega at the 1000-mb (which is equal to zero), 850-mb, 700-mb, and 500-mb levels. After differentiating with respect to pressure and setting $p = p_{1000}$ the following equation is obtained:

$$\begin{aligned} \left. \frac{\partial \omega}{\partial p} \right|_{p=1000} = & \frac{P_0^2 - P_0(P_2 + P_3) + P_2 P_3}{(P_1 - P_0)(P_1 - P_2)(P_1 - P_3)} \omega_{850} + \\ & \frac{P_0^2 - P_0(P_1 + P_3) + P_1 P_3}{(P_2 - P_0)(P_2 - P_1)(P_2 - P_3)} \omega_{700} + \quad (B-6) \\ & \frac{P_0^2 - P_0(P_1 + P_2) + P_1 P_3}{(P_3 - P_0)(P_3 - P_1)(P_3 - P_2)} \omega_{500} \end{aligned}$$

Setting in appropriate values of P_0 , P_1 , P_2 , and P_3 , the above becomes,

$$\left. \frac{\partial \omega}{\partial p} \right|_{p=1000} = -.0190476 \omega_1 + .0083333 \omega_2 \quad (B-7) \\ - .0012857 \omega_3$$

The coefficients derived above are constant with respect to time.

The values of the coefficients appearing in $\Phi(p)$ and $\frac{\partial \Phi}{\partial p}$ given by eqs. (B-4), (B-5) have been stored and employed in subroutine for generating

$$\begin{array}{ll} \Phi(p_k) & k = 1, \dots, 7 \\ \frac{\partial \Phi}{\partial p}(p_k) & k = 2, \dots, 6 \end{array}$$

In the uppermost level, i.e. for both Φ_7 and $(\Phi_p)_6$ it was found to be useful to make use of the Navy Weather Research Facility extrapolation procedure to obtain a hydrostatically-consistent best estimate for Φ_{100} .

APPENDIX C

Treatment of Horizontal Derivatives

The horizontal derivatives this paper is concerned with are the Laplacian operator, the Jacobian operator and the del-dot-del operation. The finite difference forms of these are exhibited below; the superscripts refer to the designated points exhibited in Fig. 31.

$$\text{Laplacian: } \nabla^2 A = \frac{m^2}{d^2} (A_1 + A_2 + A_3 + A_4 - 4A_0) \quad (\text{C-1})$$

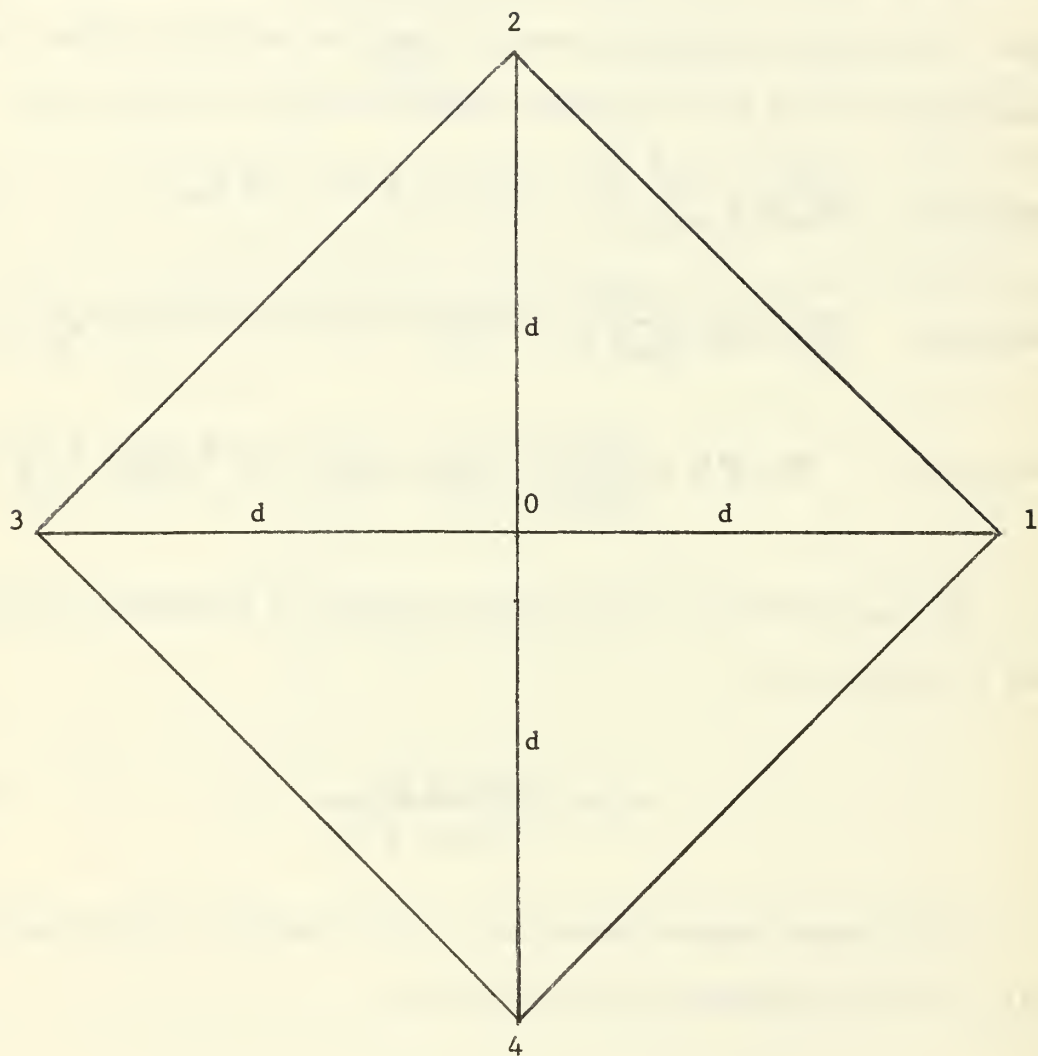
$$\text{Jacobian: } J(A, B) = \frac{m^2}{4d^2} [(A_1 - A_3)(B_2 - B_4) - (A_2 - A_4)(B_1 - B_3)] \quad (\text{C-2})$$

$$\text{Del } A \cdot \text{Del } B = \nabla A \cdot \nabla B = \frac{m^2}{4d^2} [(A_1 - A_3)(B_1 - B_3) + (A_2 - A_4)(B_2 - B_4)] \quad (\text{C-3})$$

The map factor "m" in the above equations is dependent on latitude ϕ and is expressed as:

$$m = \frac{1 + \sin \phi}{1 + \sin 60} \quad (\text{C-4})$$

The distance between gridpoints, "d" in the grid used (Figs. 2, 31), is 381 kilometers, true at 60 north.



Finite Differencing Grid

Figure 31

APPENDIX D

Computations of Static Stability Parameter

The static stability parameter, σ , at level k may be expressed as follows:

$$\sigma_k = \left(-\frac{R_d T}{p} \frac{1}{\theta} \frac{\partial \theta}{\partial p} \right)_k \quad (D-1)$$

which may be rewritten as:

$$\sigma_k = -\frac{R_d}{p^2} \left(p \frac{\partial T}{\partial p} - \frac{R_d T}{C_p} \right) \quad (D-2)$$

by use of the Poisson relationship. Using the relation

$$T = -\frac{1}{R_d} \frac{\partial \Phi}{\partial \ln p} \quad (D-3)$$

gives:

$$\sigma_k = \frac{1}{p^2} \left(\frac{\partial^2 \Phi}{\partial (\ln p)^2} - \frac{R_d}{C_p} \frac{\partial \Phi}{\partial \ln p} \right) \quad (D-4)$$

Assuming σ constant within the layer pair $(k-1, k)$, $(k, k+1)$

the previous equation is set up as an ordinary differential equation in the form

$$\frac{d^2 \Phi}{d(\ln p)^2} - \frac{R_d}{C_p} \frac{d \Phi}{d \ln p} = \sigma_k p^2 \quad (D-5)$$

The above is integrated with respect to $\ln p$ from $p_{k-\frac{1}{2}}$ to $p_{k+\frac{1}{2}}$

where these pressures are the log means for the two layers, that is:

$$p_{k-\frac{1}{2}} = (p_k p_{k-1})^{\frac{1}{2}} \quad \text{and} \quad p_{k+\frac{1}{2}} = (p_k p_{k+1})^{\frac{1}{2}}$$

After the above operation has been performed and solved for σ_k , it leads to the finite-difference form:

$$\sigma_k = \frac{2}{p'_k (p'_{k-1} - p'_{k+1})} \left\{ \frac{\Phi_{k+1} - \Phi_k}{\ln \frac{p_k}{p_{k+1}}} + \frac{\Phi_{k-1} - \Phi_k}{\ln \frac{p_{k-1}}{p_k}} + \frac{Ra}{2C_p} (\Phi_{k+1} - \Phi_{k-1}) \right\} \quad (D-6)$$

The lower bound on the braced quantity above is to be $\frac{1}{8} \frac{Ra}{2C_p} (\Phi_{k+1} - \Phi_{k-1})$ thus σ_k may be solved at all required levels.

APPENDIX E

Procedure for 100-mb Height Extrapolation

Navy Weather Research Facility (Lea, 1961) outlines a method of deriving a 100-mb extrapolated height field from the 200-mb heights and temperature fields in the form

$$Z_{100} = A_0 + A_1 Z_{200} + A_2 T_{200} \quad (\text{E-1})$$

The coefficients A_0 , A_1 , and A_2 vary with both latitude and month of the year.

The regression coefficients A_0 , A_1 , A_2 are defined for the centers of latitude belts of 10° latitude (or multiple thereof) in width. Since the A_i for one belt generally is different from that of the adjacent belt, continuity required a smooth transition from one belt into the next, which was accomplished by linear interpolation between A_i 's and the linear distance between latitude band centers.

Since temperature fields were not utilized directly in this study, the following approximation was made:

$$T = -\frac{1}{R_d} \frac{\partial \Phi}{\partial \ln p} \quad (\text{E-2})$$

Using the centered finite-difference scheme for $\frac{\partial \Phi}{\partial \ln p}$ at 200 mb, equation (E-1) becomes

$$Z_{100} = \frac{A_0 + A_1 Z_{200} - A_2 \left(\frac{\Phi_{300}}{R_d \ln 3} + 273 \right)}{\left(1 - \frac{g A_2}{R_d \ln 3} \right)} \quad (\text{E-3})$$

FORTRAN IV PROGRAM

80

```

1000 REAL*8 TI(12)
1001 DATA RE/973.71/, IP/26/, JP/26/, G/9.8/, FB/1.03E-04/, D/3.81E05/,
1002 *XI/13H OMEGA FIELDS/
1003 DATA BB/1.2E06/ 51)
1004 DIMENSION E(51, 51)
1005 DIMENSION RM(7), AA(3, 7)
1006 DIMENSION F(51, 51), FM(51, 51), ZT(51, 51), ZO(51, 51), A(51, 51), R(51, 51)
1007 1, C(51, 51), Z(51, 51), Z2(51, 51), Z3(51, 51), PSI(51, 51), PSI2(51, 51),
1008 2, PSI3(51, 51), OM1(51, 51), OM2(51, 51), OM3(51, 51)
1009 3, PSIP(51, 51), GZP(51, 51), SIG(51, 51)
1000 4, CHI1(51, 51), CHI2(51, 51), CHI3(51, 51)
1001 5, C1(7), C2(7), DO(7), DI(7), P(7), R(51, 51), CO(7),
1002 6, ZTST(51, 51), ZST(624), RO(7), FF1(7), FF2(7),
1003 7, BO(7), B1(7), B2(7)
1004 8, DIMENSION COM2(51, 51)
1005 DIMENSION IJ(51, 51)
1006 DIMENSION PS1(51, 51), PS2(51, 51), PS3(51, 51)
1007 EQUIVALENCE(R(1), R(1))
1008 FORMAT(T5, 'PSI CONVERGENCE', I5)
1009 FORMAT(T5, 'LEVEL INDICATOR', I5)
1000 FORMAT(T5, 'OMEGA CONVERGENCE', I5)
1001 FORMAT(T5, 'LOOP INDICATOR', I5)
1002 FORMAT(T5, 'NO CONVERGENCE CHI', I5)
1003 FORMAT(T5, 'PSI CONVERGENCE', I5)
1004 FORMAT(T5, 'Z CONVERGENCE', I5)
1005 ITEST=0, 1, 2, 3, 4, ETC. FOR 1ST RUN, 2ND RUN, 3RD RUN, 4TH RUN, 5TH RUN, ETC
1006 ITEST=0
1007 IF(ITEST.EQ.0) N1OR2=1
1008 IF(ITEST.NE.0) N1OR2=2
1009 IF(ITEST.EQ.0) OR, ITEST.EQ.1) ISTOP=1
1000 IF(ITEST.GT.1) ISTOP=35*(ITEST-1)+1
1001 ISTOPM=ISTOP-1
1002 IF(ISTOPM.EQ.0) ISTOPM=1
1003 IF(INAL=13
1004 DS= D*D
1005 C SET UP OCTAGONAL GRID.
1006 DO 600 I=1, 51
1007 DO 600 J=1, 51
1008 IJ(I, J)=0
1009 IF(I+J.LE.16) IJ(I, J)=1
1000 IF(I+(52-J).LE.16) IJ(I, J)=1
1001 IF(I+(52-I).LE.16) IJ(I, J)=1
1002 IF(I+J.GE.88) IJ(I, J)=1
1003 IF(I.EQ.1) OR, I.EQ.51) IJ(I, J)=1

```

```

        IF(J.EQ.1.OR.J.EQ.51) IJ(I,J)=1
        CONTINUE
        C READ VALUES OF COEFFICIENTS FOR VERTICAL DERIVATIVES.
        DO 2 K=1,7
            READ(5,1008) B0(K),B1(K),B2(K)
2         READ(5,200) C0(K),C1(K),C2(K),D0(K),D1(K),D2(K)
1008      FORMAT(1P3E13.6)
200      FORMAT(1P6E13.6)
        READ(5,201) P
201      FORMAT(7F10.0)
        N=51
        AMIN=0.0
        BZ=0.0
        IJT=0
        ICON=1
        C COMPUTE CORIOLIS PARAMETER AND MAP FACTOR.
        DO 1 I=1,51
        DO 1 J=1,51
            COM2(I,J)=0.0
            F(I,J)= (RE-((I-IP)**2+(J-JP)**2))/(RE+((I-IP)**2+(J-JP)**2))
1         FM(I,J) = 1.86603/(1.0+F(I,J))
            F(I,J)= 2.0*7.2921E-05*F(I,J)
1005      READ(5,1005) FF1,FF2,RO
            FORMAT(7F10.0)
            DO 12 L=1,39
            LL=16*L
            LF=16*L-15
            READ(5,100) (ZST(I),I=LF,LL)
12         CONTINUE
100         FORMAT(16F5.0)
            DO 402 I=1,3
            READ(5,400) (AA(I,J),J=1,7)
402         FORMAT(7F11.5)
400         READ(5,401) RM
401         FORMAT(7F10.0)
            IF(I.TEST.NE.0)GO TO 7
            READ(11) Z,TI
            READ(11) Z2,TI
            READ(11) Z3,TI
            DO 3 L=4,57
            READ(11) Z0,TI
3         READ(11) Z1,TI
7         IF(I.TEST.EQ.0)GO TO 8
            DO 6 L=1,57

```



```

6      READ(11)ZO,TI
      READ(11)ZT,TI
      DO 702 L=1,ISTOP
702    READ(14)Z
      DO 700 L=1,5
700    READ(14)Z2
      DO 701 L=1,5
701    READ(14)Z3
8      IT=12
      ITP1=IT+1
      IF(ITEST.NE.0)IT=14
      C BEGIN TIME STEP
      C DO 36C ITIME=N1OR2,IFINAL
      C SOLVE FOR DELTA Z STANDARD.
      DO 11 I=1,51
      DO 11 J=1,51
      IF(ZT(I,J).LE.1457.)ZTST(I,J)=(ZT(I,J)-7(I,J))*(1457.-111.) /
      * (Z2(I,J)-Z(I,J)) +111.
      IF(ZT(I,J).GT.1457.)ZTST(I,J)=(ZT(I,J)-72(I,J))*(3C12.-1457.) /
      * (Z3(I,J)-Z2(I,J)) +1457.
      C OBTAIN TERRAIN PRESSURE.
      DO 21 I=1,51
      DO 21 J=1,51
      DO 16 L=1,624
      IF(ZST(L)-ZTST(I,J).GT.0.0) GO TO 21
      CONTINUE
      PST(I,J)= 1050.-L+1.0
      REWIND 11
      DO 9 I=1,51
      DO 9 J=1,51
      A(I,J)=0.0
      B(I,J)=0.0
      C(I,J)=0.0
      IF(ITIME.NE.1)GO TO 19
      DO 5 K=1,7
      READ(11)Z,TI
      DO 10 I=1,51
      DO 10 J=1,51
      COM2(I,J)=C.0
      OM1(I,J)=0.0
      C COMPUTATIONS
      PSI(I,J)= G*7(I,J)/FR
      CALL LAP (Z,C,FM,DS,I,J)
      CALL MUL (C,G,C,IJ)
      L=0
      C 10

```

```

13 IND= C
CALL DDD (PSI,F,A,FM,DS,IJ)
CALL SUB(A,C,A,IJ)
CALL DIVF(A,F,A,IJ)
DO 15 I=2,50
DO 15 J=2,50
IF(IJ(I,J).EQ.1)GO TO 15
R(I,J)= PSI(I+1,J)+PSI(I-1,J)+PSI(I,J+1)+PSI(I,J-1)-4.0*PSI(I,J)
1 +DS* A(I,J)/FM(I,J)*.2
IF (ABS(R(I,J)).GT.1.0E05)IND=1
PSI(I,J)= PSI(I,J)+ 1.4*R(I,J)/4.0
CONTINUE
L=L+1
IF(L.EQ.50) GO TO 20
IF(IND.EQ.1) GO TO 13
20 WRITE(12)Z
WRITE(12)OM1
WRITE(12)PSI
WRITE(12)OM1
WRITE(12)OM1
CONTINUE
5 BEGIN ITERATIONS BETWEEN OMEGA AND CHI.
19 DO 154 LOOP=1,9
IFLAG=0
REWIND IT
DO 704 L=1,ISTOPM
READ(IT)Z )PS1
READ(IT)PSI
READ(IT)OM1 )CHI1
WRITE(ITP1)Z
WRITE(ITP1)PS1
WRITE(ITP1)PSI
WRITE(ITP1)OM1
WRITE(ITP1)CHI1
READ(IT)Z2 )PS2
READ(IT)PSI2
READ(IT)OM2 )CHI2
WRITE(ITP1)Z2
WRITE(ITP1)PS2

```

```

C START COMPUTATIONS FOR OBTAINING OMEGA AND CHI
WRITE(ITP1)PSI2
DO 54 K=2,6
  READ(IT)Z3
  READ(IT)PS3
  READ(IT)PSI3
  READ(IT)OM3
  READ(IT)CHI3
  IF(LOOP.NE.1)GO TO 40
  IF(K.NE.2)GO TO 40
C COMPUTE GEOSTROPHIC WIND.
DO 202 I=2,50
DO 202 J=2,50
  IF(IJ(I,J).EQ.1)GO TO 202
  IF(PTST(I,J).GT.875.) C(I,J)=G*SQR((Z2(I+1,J)-Z2(I-1,J))**2
  1+(Z2(I,J+1)-Z2(I,J-1))**2)*FM(I,J)/(2.0*D*F(I,J))
  1 G*SQR((Z3(I+1,J)-Z3(I-1,J))**2
  1+(Z3(I,J+1)-Z3(I,J-1))**2)*FM(I,J)/(2.0*D*F(I,J))
  IF(C(I,J).LE.0.0) WRITE(6,300) I,J
  IF(C(I,J).LE.0.0) C(I,J)=1.0
300 FORMAT(IX,2I5)
C COMPUTE DRAG COEFFICIENTS.
C(I,J)=C(I,J)*(.205/(ALOG10(ABS(C(I,J)/(F(I,J)*ZO(I,J)
  1*(.01)))-.556))**2
202 CONTINUE
C COMPUTE RELATIVE VORTICITY.
DO 500 I=2,50
DO 500 J=2,50
  IF(IJ(I,J).EQ.1)GO TO 500
  IF(PTST(I,J).GT.875.) A(I,J)=
  1FM(I,J)**2*(PSI2(I-1,J)+PSI2(I,J+1)+PSI2(I,J-1)
  2-4.0*PSI2(I,J))/DS
  1 IF(PTST(I,J).LE.875.) A(I,J)=
  1 FM(I,J)**2*(PSI3(I-1,J)+PSI3(I,J+1)+PSI3(I,J-1)
  2-4.0*PSI3(I,J))/DS
500 CONTINUE
CALL MULF(A,C,A,IJ)
C COMPUTE DEL Z DOT DEL C SUB D TIMES VG.
DO 501 I=2,50
DO 501 J=2,50
  IF(IJ(I,J).EQ.1)GO TO 501
  IF(PTST(I,J).GT.875.) B(I,J)= FM(I,J)**2*((Z2(I+1,J)-Z2(I-1,J))
  1*(C(I+1,J)-C(I-1,J))+ (Z2(I,J+1)-Z2(I,J-1))*(C(I,J+1)-C(I,J-1))
  2/(4.0*DS)

```

```

501 IF (PTST(I,J).LE.875.)B(I,J)=FM(I,J)**2*((Z3(I+1,J)-Z3(I-1,J))*
1 (C(I+1,J)-C(I-1,J))+(Z3(I,J+1)-Z3(I,J-1))*C(I,J+1)-C(I,J-1))
2 /(4.0*DS)
CONTINUE
CALL MUL(B,G,B,IJ)
CALL DIVF(B,F,B,IJ)
CALL ADD(A,B,A,IJ)
CALL DIVF(A,F,A,IJ)
DO 502 I=2,50
DO 502 J=2,50
IF(IJ(I,J).EQ.1)GO TO 502
IF(PTST(I,J).GT.875.)A(I,J)=A(I,J)*RO(2) *.01
IF(PTST(I,J).LE.875.)A(I,J)=A(I,J)*RO(3) *.01
CONTINUE TERRAIN TERM.
C COMPUTE
DO 503 I=2,50
DO 503 J=2,50
IF(IJ(I,J).EQ.1)GO TO 503
IF(PTST(I,J).GT.875.)B(I,J)=FM(I,J)**2*((Z2(I+1,J)-Z2(I-1,J))*
1 (PTST(I,J+1)-PTST(I,J-1))-(Z2(I,J+1)-Z2(I,J-1))*PTST(I+1,J)-
2 PTST(I-1,J)))/(4.0*DS)
IF(PTST(I,J).LE.875.)B(I,J)=FM(I,J)**2*((Z3(I+1,J)-Z3(I-1,J))*
1 (PTST(I,J+1)-PTST(I,J-1))-(Z3(I,J+1)-Z3(I,J-1))*PTST(I+1,J)
2 -PTST(I-1,J)))/(4.0*DS)
CONTINUE
CALL DIVF(B,F,B,IJ)
CALL SUB(B,A,A,IJ)
CALL MUL(A,G,COM2,IJ)
C WE HAVE COMPLETED SOLUTION OF OMEGA L0.
C COMPUTE STATIC STABILITY PARAMETER.
DO 45 I=1,51
DO 45 J=1,51
SIG(I,J)=2.0/(P(K)*(P(K-1)-P(K+1)))*G*(
*(Z3(I,J)-Z2(I,J))/ALOG(P(K)/P(K+1)))+
*(Z(I,J)-Z(I,J))/ALOG(P(K-1)/P(K)) +
*0.143*(Z3(I,J)-Z(I,J))
IF(SIG(I,J)*P(K)*(P(K-1)-P(K+1))/2.0.LE.G*(Z3(I,J)-Z(I,J))*
*Z(I,J))*0.143/8.0
SIG(I,J)=G*(Z3(I,J)-Z(I,J))*
*0.143/8.0
**2.0/(P(K)*(P(K-1)-P(K+1)))
CONTINUE
C COMPUTE VERTICAL DERIVATIVES OF PSI AND PHI.
DO 53 I=1,51
DO 53 J=1,51
PSIP(I,J)=(CO(K)*PSI(I,J)+C1(K)*PSI2(I,J)+C2(K)*PSI3

```

```

53      * ( GZP( I,J))/P(K)
61      */P(K)
      I,J)=G*(CO(K)*Z ( I,J)+C1(K)*Z2( I,J)+C2(K)*Z3( I,J))
      CALL LAP(PSI2,A,FM,DS,IJ)
      CALL ADD(A,FA,IJ)
      CALL JAC(PSIP,A,C,FM,DS,IJ)
      CALL LAP(PSIP,B,FM,DS,IJ)
      CALL JAC(PSI2,B,A,FM,DS,IJ)
      CALL ADD(A,CA,IJ)
      CALL MULF(A,FA,IJ)
      CALL JAC(PSI2,GZP,B,FM,DS,IJ)
      CALL LAP(B,C,FM,DS,IJ)
      CALL SUB(A,CA,IJ)
      IF(L OOP.EQ.1.AND. I TIME.EQ.1)GO TO 63
      CALL DDD(CHI2,GZP,C,FM,DS,IJ)
      CALL LAP(C,B,FM,DS,IJ)
      CALL SUB(A,B,A,IJ)
      CALL JAC(PSI2,GZP,C,FM,DS,IJ)
      CALL DDD(CHI2,GZP,B,FM,DS,IJ)
      CALL ADD(B,C,B,IJ)
DO 94 I=1,51
DO 94 J=1,51
      PSIP NOW WILL BE SIG*OM
      IF(PTST(I,J).GT.875)PSIP(I,J)=SIG(I,J)*(OM2(I,J)+FF1(K)*COM2(I,J))
      IF(PTST(I,J).LE.875)PSIP(I,J)=SIG(I,J)*(OM2(I,J)+FF2(K)*COM2(I,J))
      GZP (I,J)=PSIP(I,J)-SIG(I,J)*OM2(I,J)
      GZP NOW SIG*CAP OMEGA
      CONTINUE
      CALL LAP (GZP ,B,FM,DS, IJ)
      CALL SUB (A,B,A,IJ)
      CALL ADD(PSIP,B,B,IJ)
      CALL DDD(F,B,GZP,FM,DS,IJ)
      GZP NOW WILL EQUAL DEL F . DEL PHIPT
      CALL DIV(GZP,F,B,IJ)
      CALL ADD(A,B,A,IJ)
DO 210 I=2,50
DO 210 J=2,50
      IF(IJ(I,J).EQ.1)GO TO 210
      IF(PTST(I,J).GT.875.0) A(I,J)= A(I,J)- F(I,J)**2
      1 *COM2 (I,J) (I,J)*(DO(K)*FF1(K-1)+D1(K)*FF1(K)+D2(K)*FF1(K+1))
      1 IF(PTST(I,J).LE.875.0) A(I,J)= A(I,J)- F(I,J)**2
      1 *COM2 (I,J) (I,J)*(DO(K)*FF2(K-1)+D1(K)*FF2(K)+D2(K)*FF2(K+1))
      CONTINUE
      WRITE(6,1001)K
63      COMPLETE SOLUTION OF FORCING FUNCTION FOR OMEGA EQUATION.
C

```



```

C      BEGIN RELAXATION OF OMEGA EQUATION.
DO 64 I=1,51
DO 64 J=1,51
E(I,J)=OM2(I,J)
DO 68 LL=1,20
IND=0
DO 60 I=2,50
DO 60 J=2,50
IF(IJ(I,J).EQ.1)GO TO 60
R(I,J)=OM2(I+1,J)*SIG(I+1,J)+OM2(I-1,J)*SIG(I-1,J)+
U OM2(I,J+1)*SIG(I,J+1)+OM2(I,J-1)*SIG(I,J-1)-4.0*OM2(I,J)
2 *SIG(I,J)+(F(I,J)-DS*(DO(K)*OM1(I,J))/FM(I,J))**2
3 D2(K)*OM3(I,J))-DS*A(I,J))/FM(I,J))**2
IF(ABS(R(I,J)).GT.1.0E-06)IND=1
OM2(I,J)=OM2(I,J)+R(I,J)/(4.0*SIG(I,J)-DS*F(I,J)**2*
1 DI(K)/FM(I,J)**2)*I.3
1 CONTINUE
IF(IND.EQ.0)GO TO 69
60 CONTINUE
68 CONTINUE
DO 67 I=2,50
DO 67 J=2,50
IF(IJ(I,J).EQ.1)GO TO 67
C      COMPARE THE NEW OMEGA WITH ONE FROM LAST PASS.
IF(ABS(E(I,J)-OM2(I,J)).GT.2.0E-04)IFLAG=1
67 CONTINUE
WRITE(6,1002)LL
L=0
IND=0
DO 90 I=2,50
DO 90 J=2,50
IF(IJ(I,J).EQ.1)GO TO 90
IF(PTST(I,J).GT.875.)COM=COM2(I,J)*(FF1(K-1)*BC(K)+FF1(K)*B1(K)
1+FF1(K+1)*B2(K))
IF(PTST(I,J).LE.875.)COM=COM2(I,J)*(FF2(K-1)*HC(K)+FF2(K)*B1(K)
1+FF2(K+1)*B2(K))
R(I,J)=CHI2(I+1,J)+CHI2(I-1,J)+CHI2(I,J+1)+CHI2(I,J-1)
2 -4.0*CHI2(I,J)+DS*(B0(K)*OM1(I,J)+B1(K)*OM2(I,J))**2
+ B2(K)*OM3(I,J)+COM)/FM(I,J))**2
IF(ABS(R(I,J)).GT.5.0E-04)IND=1
CHI2(I,J)=CHI2(I,J)+1.4*R(I,J)/4.0
CONTINUE
L=L+1
90 IF(L.EQ.50)GO TO 91
IF(IND.EQ.1)GO TO 92
91 WRITE(6,1004)L

```

```

BND=1.0E06
AZ=1.0E-07
DO 65 I=1,51
DO 65 J=1,51
Z(I,J)=Z2(I,J) ( I,J)
PSI1(I,J)=PSI2(I,J) ( I,J)
PSI2(I,J)=PSI3(I,J) ( I,J)
CHI1(I,J)=CHI2(I,J) ( I,J)
CHI2(I,J)=CHI3(I,J) ( I,J)
OM1(I,J)=OM2(I,J) ( I,J)
OM2(I,J)=OM3(I,J) ( I,J)
WRITE(ITP1)OM1
WRITE(ITP1)CHI1
WRITE(ITP1)Z2
WRITE(ITP1)PSI3
WRITE(ITP1)PSI2
CONTINUE
TEMP=IT
ITP1=ITP1+1
IF(TEMP.EQ.14)ITP1=12
WRITE(IT)OM2
WRITE(IT)CHI2
IF(IFLAG.EQ.0)GO TO 155
154 CONTINUE
C COMPLETE PASS ON OMEGA AND CHI.ONCE OUT OF THIS LOOP COMMENCE
C PROGNOSTIC STEP.
155 REWIND IT
WRITE(6,1003)LOOP
DO 299 ITP1
REWIND ITP1
DO 299 LL=1,5
READ(IT)CHI1
DO 304 LL=1,4
READ(IT)OM1
DO 301 LL=1,5
READ(IT)OM2
DO 302 LL=1,5
READ(IT)OM3
DO 325 L=1,50
IND=0
C COMPUTE PARTIAL OMEGA RE PRESSURE AT 1000 MB.
DO 303 I=2,50
DO 303 J=2,50
IF(IJ(I,J).EQ.1)GO TO 303

```

```

C(I,J)=(-.0190476)*OM1(I,J)+.00833333*OM2(I,J)-.0012857*OM3(I,J)
IF(PTST(I,J).GT.875.0)C(I,J)=
$   +FF1(4)*(-.0012857))*COM2(I,J)+C(I,J)
*   IF(PTST(I,J).LE.875.0)C(I,J)=
*   +FF2(4)*(-.0012857))*COM2(I,J)+C(I,J)
C   OBTAIN CHI AT 1000 MB.
R(I,J)=CHI(I+1,J)+CHI(I-1,J)+CHI(I,J+1)+CHI(I,J-1)
*   -4.0*CHI(I,J)+DS*C(I,J)/FM(I,J)**2
CHI(I,J)=CHI(I,J)+1.4*R(I,J)/4.0
IF(ABS(R(I,J)).GT.5.0E 04)IND=1
CONTINUE
303 IF(IND.EQ.0)GO TO 326
325 CONTINUE
326 WRITE(6,1004)
REWIND IT
READ (IT) Z
READ (IT) PSI
READ (IT) PSI
READ (IT) OM1
READ (IT) A
READ (IT) Z2
READ (IT) PSI2
READ (IT) OM2
READ (IT) CHI2
DO 351 K=1,6 GO TO 307
IF(K.EQ.2)GO TO 307
READ (IT) Z3
READ (IT) PSI3
READ (IT) OM3
READ (IT) CHI3
IF(K.EQ.1)GO TO 309
307 COMPUTE PARTIAL OMEGA RE PRESSURE AT ALL OTHER LEVELS.
DO 308 I=2,50
DO 308 J=2,50
IF(IJ(I,J).EQ.1)GO TO 308
C(I,J)=B0(K)*OM1(I,J)+B1(K)*OM2(I,J)+B2(K)*OM3(I,J)
308 CONTINUE
C   OBTAIN PARTIAL CAP OMEGA RE PRESSURE.
DO 311 I=2,50
DO 311 J=2,50
IF(IJ(I,J).EQ.1)GO TO 311

```

```

310 IF(PTST(I,J).GT.875.0)A(I,J)=
*      (FF1(K-1)*B0(K)+FF1(K)*B1(K)+FF1(K+1)
*      *B2(K))*COM2(I,J)
* IF(PTST(I,J).LE.875.0)A(I,J)=
*      (FF2(K-1)*B0(K)+FF2(K)*B1(K)+FF2(K+1)
*      *B2(K))*COM2(I,J)
311 CONTINUE
CALL ADD (C,A,C,IJ)
CALL MULF(F,C,A,IJ)
309 IF(K.EQ.1)GO TO 316
DO 315 I=1,51
DO 315 J=1,51
PSI(I,J)=PSI2(I,J)
PSI(I,J)=PS2(I,J)
CHI1(I,J)=CHI2(I,J)
Z(I,J)=Z2(I,J)
315 CONTINUE
C COMPUTE SMOOTHING TERM.
316 IF(I.TIME.EQ.1)CALL LAP(PSI,C,FM,DS,IJ)
IF(I.TIME.NE.1)CALL LAP(PSI,C,FM,DS,IJ)
CALL LAP (C ,B,FM,DS,IJ)
CALL MUL (B ,BB,B,IJ)
CALL ADD (A,B,A,IJ)
CALL DDD (CHI1,F,B,FM,DS,IJ)
CALL SUB (B,A,A,IJ)
CALL LAP(PSI,C,FM,DS,IJ)
CALL ADD (C,F,C,IJ)
CALL JAC (PSI,C,B,FM,DS,IJ)
CALL ADD (B,A,A,IJ)
DO 320 I=1,51
DO 320 J=1,51
C(I,J)=0.C
320 RELAX DO 335 L=1,50
C IND=0
DO 330 I=2,50
DO 330 J=2,50
IF(IJ(I,J).EQ.1)GO TO 330
R(I,J)=C(I+1,J)+C(I-1,J)+C(I,J+1)+C(I,J-1)-C(I,J)*4.0+DS*A(I,J)
*      /FM(I,J)*#2
C(I,J)=C(I,J)+1.4*R(I,J)/4.0
330 IF(ABS(R(I,J)).GT.9.0)IND=1
CONTINUE
IF(IND.EQ.0)GO TO 336
CONTINUE

```

```

336 WRITE(6,1006) L
    IF(ITIME.EQ.1) DELT=1800.
    IF(ITIME.EQ.2) DELT=3600.
    IF(ITIME.GT.2) DELT=7200.
    IF(ITEST.NE.0) DELT=7200.
    CALL MUL(C,DELT,C,IJ)
    C OBTAIN NEW VALUE FOR PSI.
    DO 337 I=1,51
    DO 337 J=1,51
    IF(ITIME.EQ.1) C(I,J)=C(I,J)+PSI(I,J)
    IF(ITIME.NE.1) C(I,J)=C(I,J)+PSI(I,J)
    CALL LAP(C,A,FM,DS,IJ)
    CALL MUL(F,A,F,A,IJ)
    CALL DDD(F,C,B,FM,DS,IJ)
    CALL ADD(A,B,A,IJ)
    CALL DIV(A,G,A,IJ)
    C SOLVE BALANCE EQUATION FOR NEW HEIGHTS.
    DO 341 L=1,50
    IND=0
    DO 340 I=2,50
    DO 340 J=2,50
    IF(IJ(I,J).EQ.1) GO TO 340
    R(I,J)=Z(I+1,J)+Z(I,J+1)+Z(I,J-1) -4.0*Z(I,J)
    1 -DS*A(I,J)/FM(I,J)**2
    IF(ABS(R(I,J)).GT.1.5) IND=1
    Z(I,J)=Z(I,J)+1.3*R(I,J)/4.0
    CONTINUE
    IF(IND.EQ.0) GO TO 342
    CONTINUE
    WRITE(6,1007) L
    IF(ITIME.EQ.1) ITP1=14
    WRITE(ITP1) Z
    IF(ITEST.EQ.0) AND. ITIME.EQ.2) WRITE(ITP1) PSI
    IF(ITEST.NE.0) OR. ITIME.NE.2) WRITE(ITP1) PSI
    WRITE(ITP1) C
    IF(K.EQ.1) WRITE(ITP1) OM1
    IF(K.GT.1) WRITE(ITP1) OM2
    WRITE(ITP1) CH11
    IF(ITIME.NE.13) GO TO 344
    BND=60.0
    AZ=.001
    IF(K.EQ.5) CALL METMAP(Z,M,N,XI,BND,AZ,BZ,AMIN,IJT,ICON)
    IF(K.EQ.1) OR. K.EQ.4) CALL METMAP(Z,N,M,XI,BND,AZ,BZ,AMIN,IJT,
    1 ICON)
    DO 380 I=1,51
344

```


93

```

410      Z3(I,J) = (A(I,J) + B(I,J)*Z2(I,J) - C(I,J)*
1      (G*PSIP(I,J)/(286.0*1.09861) + 273.0)) /
2      (1.0 - G*C(I,J)/(286.0*1.09861))
      DO 450 I=1,51
      DO 450 J=1,51
450      PSI3(I,J)=G*Z3(I,J)/F8
      CALL LAP(Z3,C,FM,DS,IJ)
      CALL MUL(C,G,C,IJ)
C      SOLVE BALANCE FOR NEW 100 MB. PSI.
      DO 440 L=1,50
      IND=0
      DDD(PSI3,F,A,FM,DS,IJ)
      CALL SUB(A,C,F,A,IJ)
      CALL DIVF(A,F,A,IJ)
      DO 445 I=2,50
      DO 445 J=2,50
      IF(I,J,I,J).EQ.1) GO TO 445
      R(I,J)= PSI3(I+1,J)+PSI3(I-1,J)+PSI3(I,J+1)+PSI3(I,J-1)
      * -4.0*PSI3(I,J)+DS*A(I,J)/FM(I,J)**2
      IF(ABS(R(I,J)).GT.1.0E05) IND=1
      PSI3(I,J)= PSI3(I,J) + 1.4*R(I,J)/4.0
      CONTINUE
445      IF(IND.EQ.0) GO TO 446
      CONTINUE
440      WRITE(ITPL) Z3
446      WRITE(ITPL) PSI3
      WRITE(ITPL) OM3
      WRITE(ITPL) CHI3
      IF(ITIME.EQ. IFINAL) GO TO 360
      REWIND ITPL
      DO 370 L=1,5
      READ(ITPL) Z
      DO 371 L=1,5
      READ(ITPL) Z
      DO 371 L=1,5
      READ(ITPL) Z
      TEMP=IT
      IT=ITPL
      ITPL=TEMP
      CONTINUE
360      END

```

```

SUBROUTINE RES(A)
DIMENSION A(51,51)
IMAX=2
JMAX=2
RMAX=A(2,2)
DO 1 I=2,50
DO 1 J=2,50
IF(ABS(A(I,J)) .GT. ABS(RMAX)) GO TO 2
CONTINUE
WRITE(6,3) RMAX,IMAX,JMAX
FORMAT(1X,T5,'MAX RESIDUAL',1PE20.6,2I5)
RETURN
RMAX=A(I,J)
IMAX=I
JMAX=J
GO TO 1
END

```

1
3
2

```

SUBROUTINE DIVF(A,B,C,IJ)
DIMENSION A(51,51),B(51,51),C(51,51)
DIMENSION IJ(51,51)
DO 10 J=2,50
DO 10 I=2,50
IF(IJ(I,J).EQ.1)GO TO 10
C(I,J)=A(I,J)/B(I,J)
CONTINUE
RETURN
END

```

10

```

SUBROUTINE JAC (A,B,C,FM,DS,IJ)
DIMENSION A(51,51),B(51,51),C(51,51),FM(51,51)
DIMENSION IJ(51,51)
DO 10 J=2,50
DO 10 I=2,50
IF(IJ(I,J).EQ.1)GO TO 10
C(I,J)=FM(I,J)*2*((A(I+1,J)-A(I-1,J))*(B(I,J+1)-B(I,J-1))-
*(A(I,J+1)-A(I,J-1))*(B(I+1,J)-B(I-1,J)))/(4.0*DS)
CONTINUE
RETURN
END

```

10

```

SUBROUTINE MULF(A,B,C,I,J)
DIMENSION A(51,51),B(51,51),C(51,51)
DO 10 I=2,50
DO 10 J=2,50
IF(IJ(I,J).EQ.1)GO TO 10
C(I,J)=A(I,J)*B(I,J)
CONTINUE
RETURN
END

```

10

```

SUBROUTINE DIV(A,X,C,I,J)
DIMENSION A(51,51),C(51,51)
DO 10 I=2,50
DO 10 J=2,50
IF(IJ(I,J).EQ.1)GO TO 10
C(I,J)=A(I,J)/X
CONTINUE
RETURN
END

```

10

```

SUBROUTINE MUL (A,X,C,I,J)
DIMENSION A(51,51),C(51,51)
DO 10 I=2,50
DO 10 J=2,50
IF(IJ(I,J).EQ.1)GO TO 10
C(I,J)=X*A(I,J)
CONTINUE
RETURN
END

```

10

```

SUBROUTINE DDD (A,B,C,FM,DS,IJ)
  DIMENSION IJ(51,51)
  DIMENSION A(51,51),B(51,51),C(51,51),FM(51,51)
  DO 10 I=2,50
    DO 10 J=2,50
      IF(IJ(I,J).EQ.1)GO TO 10
      C(I,J)=FM(I,J)**2*((A(I+1,J)-A(I-1,J))*(B(I+1,J)-B(I-1,J))+
      *(A(I,J+1)-A(I,J-1))*(B(I,J+1)-B(I,J-1)))/(4.*C*DS)
    CONTINUE
  RETURN
END

```

10

```

SUBROUTINE LAP (A,C,FM,DS,IJ)
  DIMENSION IJ(51,51)
  DIMENSION A(51,51),C(51,51),FM(51,51)
  DO 10 I=2,50
    DO 10 J=2,50
      IF(IJ(I,J).EQ.1)GO TO 10
      C(I,J)=FM(I,J)**2*(A(I+1,J)+A(I-1,J)+A(I,J-1)+A(I,J+1))-
      *4.*A(I,J)/DS
    CONTINUE
  RETURN
END

```

10

```

SUBROUTINE SUB (A,B,C,IJ)
  DIMENSION IJ(51,51)
  DIMENSION A(51,51),B(51,51),C(51,51)
  DO 10 I=2,50
    DO 10 J=2,50
      IF(IJ(I,J).EQ.1)GO TO 10
      C(I,J)=A(I,J)-B(I,J)
    CONTINUE
  RETURN
END

```

10


```

SUBROUTINE ADD (A,B,C,IJ)
DIMENSION IJ(51,51)
DIMENSION A(51,51),B(51,51),C(51,51)
DO 10 I=2,50
DO 10 J=2,50
IF(IJ(I,J).EQ.1)GO TO 10
C(I,J)=A(I,J)+B(I,J)
CONTINUE
RETURN
END

```

10

TAPE AND DISK CONTROL CARDS FOLLOW

```

//GO.FT11F001 DD UNIT=2400,VOLUME=SER=NPS131,DSNAME=FNWFTP5,DISP=OLD *
//GO.FT12F001 DD UNIT=2311,VOLUME=SER=SCRCH1,DISP=OLD *
//DISP=(,DELETE),SPACE=(CYL,(100,2)) *
//GO.FT13F001 DD UNIT=2311,VOLUME=SER=SCRCH2,DISP=OLD *
//DISP=(,DELETE),SPACE=(CYL,(100,2)) *
//GO.FT14F001 DD UNIT=2400,VOLUME=SER=NPS115,DSNAME=BILL,DISP=(NEW,KEEP) *
//GO.SYSIN DD *

```

DATA CARDS FOLLOW

C DATA ORIGINALLY IN COLS. 73-80 OMITTED DUE TO SPACE LIMITATIONS.

```

0.0 0.0 0.0 0.0 0.0
0.0 0.0 0.0 0.0 0.0
3.333333E-03 0.0 0.0 -3.333333E-03 0.0

```

3.349463E	00-1.002641E	00-2.346837E	00-3.346837E	00-4.444443E	00-5.888888E	00-6.4.4444
3.809524E	-03-1.666666E	-03-2.142857E	-03-3.142857E	-03-4.444443E	-03-5.888888E	-03-6.4.4444
3.265949E	00-2.178493E	00-1.087457E	00-2.178493E	00-3.809523E	00-4.666666E	00-5.2.8571
2.500000E	-03-0.0	-03-2.500000E	-03-3.500000E	-03-4.444443E	-03-5.888888E	-03-6.4.4444
1.791791E	00-1.014400E	00-2.773938E	00-3.773938E	00-4.444443E	00-5.888888E	00-6.4.4444
1.666666E	-03-5.000000E	-03-6.666666E	-03-7.666666E	-03-8.666666E	-03-9.666666E	-03-10.666666E
8.662592E	-01-5.086868E	-01-1.374947E	-01-2.374947E	-01-3.374947E	-01-4.374947E	-01-5.374947E
1.000000E	-03-0.0	-03-2.000000E	-03-3.000000E	-03-4.000000E	-03-5.000000E	-03-6.000000E
1.556065E	00-1.023607E	00-2.324560E	00-3.324560E	00-4.324560E	00-5.324560E	00-6.324560E
0.0	0.0	0.0	0.0	0.0	0.0	0.0
1000.	700.	500.	300.	200.	100.	0.0
1.2133	1.0634	2.0763	1.0634	2.0763	1.0634	2.0763
-302.	-293.	-163.	-155.	-147.	-139.	-130.
-39.	-31.	-102.	-111.	-123.	-135.	-147.
29.	102.	238.	375.	514.	655.	793.
366.	514.	655.	793.	934.	1075.	1216.
505.	646.	789.	934.	1075.	1216.	1357.
789.	934.	1075.	1216.	1357.	1498.	1639.
934.	1075.	1216.	1357.	1498.	1639.	1780.
1075.	1216.	1357.	1498.	1639.	1780.	1921.
1216.	1357.	1498.	1639.	1780.	1921.	2062.
1357.	1498.	1639.	1780.	1921.	2062.	2203.
1498.	1639.	1780.	1921.	2062.	2203.	2344.
1639.	1780.	1921.	2062.	2203.	2344.	2485.
1780.	1921.	2062.	2203.	2344.	2485.	2626.
1921.	2062.	2203.	2344.	2485.	2626.	2767.
2062.	2203.	2344.	2485.	2626.	2767.	2908.
2203.	2344.	2485.	2626.	2767.	2908.	3049.
2344.	2485.	2626.	2767.	2908.	3049.	3190.
2485.	2626.	2767.	2908.	3049.	3190.	3331.
2626.	2767.	2908.	3049.	3190.	3331.	3472.
2767.	2908.	3049.	3190.	3331.	3472.	3613.
2908.	3049.	3190.	3331.	3472.	3613.	3754.
3049.	3190.	3331.	3472.	3613.	3754.	3895.
3190.	3331.	3472.	3613.	3754.	3895.	4036.
3331.	3472.	3613.	3754.	3895.	4036.	4177.
3472.	3613.	3754.	3895.	4036.	4177.	4318.
3613.	3754.	3895.	4036.	4177.	4318.	4459.
3754.	3895.	4036.	4177.	4318.	4459.	4600.
3895.	4036.	4177.	4318.	4459.	4600.	4741.
4036.	4177.	4318.	4459.	4600.	4741.	4882.
4177.	4318.	4459.	4600.	4741.	4882.	5023.
4318.	4459.	4600.	4741.	4882.	5023.	5164.
4459.	4600.	4741.	4882.	5023.	5164.	5305.
4600.	4741.	4882.	5023.	5164.	5305.	5446.
4741.	4882.	5023.	5164.	5305.	5446.	5587.
4882.	5023.	5164.	5305.	5446.	5587.	5728.
5023.	5164.	5305.	5446.	5587.	5728.	5869.
5164.	5305.	5446.	5587.	5728.	5869.	6010.
5305.	5446.	5587.	5728.	5869.	6010.	6151.
5446.	5587.	5728.	5869.	6010.	6151.	6292.
5587.	5728.	5869.	6010.	6151.	6292.	6433.
5728.	5869.	6010.	6151.	6292.	6433.	6574.
5869.	6010.	6151.	6292.	6433.	6574.	6715.
6010.	6151.	6292.	6433.	6574.	6715.	6856.
6151.	6292.	6433.	6574.	6715.	6856.	6997.
6292.	6433.	6574.	6715.	6856.	6997.	7138.
6433.	6574.	6715.	6856.	6997.	7138.	7279.
6574.	6715.	6856.	6997.	7138.	7279.	7420.
6715.	6856.	6997.	7138.	7279.	7420.	7561.
6856.	6997.	7138.	7279.	7420.	7561.	7702.
6997.	7138.	7279.	7420.	7561.	7702.	7843.
7138.	7279.	7420.	7561.	7702.	7843.	7984.
7279.	7420.	7561.	7702.	7843.	7984.	8125.
7420.	7561.	7702.	7843.	7984.	8125.	8266.
7561.	7702.	7843.	7984.	8125.	8266.	8407.
7702.	7843.	7984.	8125.	8266.	8407.	8548.
7843.	7984.	8125.	8266.	8407.	8548.	8689.
7984.	8125.	8266.	8407.	8548.	8689.	8830.
8125.	8266.	8407.	8548.	8689.	8830.	8971.
8266.	8407.	8548.	8689.	8830.	8971.	9112.
8407.	8548.	8689.	8830.	8971.	9112.	9253.
8548.	8689.	8830.	8971.	9112.	9253.	9394.
8689.	8830.	8971.	9112.	9253.	9394.	9535.
8830.	8971.	9112.	9253.	9394.	9535.	9676.
8971.	9112.	9253.	9394.	9535.	9676.	9817.
9112.	9253.	9394.	9535.	9676.	9817.	9958.
9253.	9394.	9535.	9676.	9817.	9958.	10099.
9394.	9535.	9676.	9817.	9958.	10099.	10240.
9535.	9676.	9817.	9958.	10099.	10240.	10381.
9676.	9817.	9958.	10099.	10240.	10381.	10522.
9817.	9958.	10099.	10240.	10381.	10522.	10663.
9958.	10099.	10240.	10381.	10522.	10663.	10804.
10099.	10240.	10381.	10522.	10663.	10804.	10945.
10240.	10381.	10522.	10663.	10804.	10945.	11086.
10381.	10522.	10663.	10804.	10945.	11086.	11227.
10522.	10663.	10804.	10945.	11086.	11227.	11368.
10663.	10804.	10945.	11086.	11227.	11368.	11509.
10804.	10945.	11086.	11227.	11368.	11509.	11650.
10945.	11086.	11227.	11368.	11509.	11650.	11791.
11086.	11227.	11368.	11509.	11650.	11791.	11932.
11227.	11368.	11509.	11650.	11791.	11932.	12073.
11368.	11509.	11650.	11791.	11932.	12073.	12214.
11509.	11650.	11791.	11932.	12073.	12214.	12355.
11650.	11791.	11932.	12073.	12214.	12355.	12496.
11791.	11932.	12073.	12214.	12355.	12496.	12637.
11932.	12073.	12214.	12355.	12496.	12637.	12778.
12073.	12214.	12355.	12496.	12637.	12778.	12919.
12214.	12355.	12496.	12637.	12778.	12919.	13060.
12355.	12496.	12637.	12778.	12919.	13060.	13201.
12496.	12637.	12778.	12919.	13060.	13201.	13342.
12637.	12778.	12919.	13060.	13201.	13342.	13483.
12778.	12919.	13060.	13201.	13342.	13483.	13624.
12919.	13060.	13201.	13342.	13483.	13624.	13765.
13060.	13201.	13342.	13483.	13624.	13765.	13906.
13201.	13342.	13483.	13624.	13765.	13906.	14047.
13342.	13483.	13624.	13765.	13906.	14047.	14188.
13483.	13624.	13765.	13906.	14047.	14188.	14329.
13624.	13765.	13906.	14047.	14188.	14329.	14470.
13765.	13906.	14047.	14188.	14329.	14470.	14611.
13906.	14047.	14188.	14329.	14470.	14611.	14752.
14047.	14188.	14329.	14470.	14611.	14752.	14893.
14188.	14329.	14470.	14611.	14752.	14893.	15034.
14329.	14470.	14611.	14752.	14893.	15034.	15175.
14470.	14611.	14752.	14893.	15034.	15175.	15316.
14611.	14752.	14893.	15034.	15175.	15316.	15457.
14752.	14893.	15034.	15175.	15316.	15457.	15598.
14893.	15034.	15175.	15316.	15457.	15598.	15739.
15034.	15175.	15316.	15457.	15598.	15739.	15880.
15175.	15316.	15457.	15598.	15739.	15880.	16021.
15316.	15457.	15598.	15739.	15880.	16021.	16162.
15457.	15598.	15739.	15880.	16021.	16162.	16303.
15598.	15739.	15880.	16021.	16162.	16303.	16444.
15739.	15880.	16021.	16162.	16303.	16444.	16585.
15880.	16021.	16162.	16303.	16444.	16585.	16726.
16021.	16162.	16303.	16444.	16585.	16726.	16867.
16162.	16303.	16444.	16585.	16726.	16867.	17008.
16303.	16444.	16585.	16726.	16867.	17008.	17149.
16444.	16585.	16726.	16867.	17008.	17149.	17290.
16585.	16726.	16867.	17008.	17149.	17290.	17431.
16726.	16867.	17008.	17149.	17290.	17431.	17572.
16867.	17008.	17149.	17290.	17431.	17572.	17713.
17008.	17149.	17290.	17431.	17572.	17713.	17854.
17149.	17290.	17431.	17572.	17713.	17854.	17995.
17290.	17431.	17572.	17713.	17854.	17995.	18136.
17431.	17572.	17713.	17854.	17995.	18136.	18277.
17572.	17713.	17854.	17995.	18136.	18277.	18418.
17713.	17854.	17995.	18136.	18277.	18418.	18559.
17854.	17995.	18136.	18277.	18418.	18559.	18690.
17995.	18136.	18277.	18418.	18559.	18690.	18831.
18136.	18277.	18418.	18559.	18690.	18831.	18972.
18277.	18418.	18559.	18690.	18831.	18972.	19113.
18418.	18559.	18690.	18831.	18972.	19113.	19254.
18559.	18690.	18831.	18972.	19113.	19254.	19395.
18690.	18831.	18972.	19113.	19254.	19395.	19536.
18831.	18972.	19113.	19254.	19395.	19536.	19677.
18972.	19113.	19254.	19395.	19536.	19677.	19818.
19113.	19254.	19395.	19536.	19677.	19818.	19959.
19254.	19395.	19536.	19677.	19818.	19959.	20100.
19395.	19536.	19677.	19818.	19959.	20100.	20241.
19536.	19677.	19818.	19959.	20100.	20241.	20382.
19677.	19818.	19959.	20100.	20241.	20382.	20523.
19818.	19959.	20100.	20241.	20382.	20523.	20664.
19959.	20100.	20241.	20382.	20523.	20664.	20805.
20100.	20241.	20382.	20523.	20664.	20805.	20946.
20241.	20382.	20523.	20664.	20805.	20946.	21087.
20382.	20523.	20664.	20805.	20946.	21087.	21228.
20523.	20664.	20805.	20946.	21087.	21228.	21369.
20664.	20805.	20946.	21087.	21228.	21369.	21510.
20805.	20946.	21087.	21228.	21369.	21510.	21651.
20946.	21087.	21228.	21369.	21510.	21651.	21792.
21087.	21228.	21369.	21510.	21651.	21792.	21933.
21228.	21369.	21510.	21651.	21792.	21933.	22074.
21369.	21510.	21651.	21792.	21933.	22074.	22215.
21510.	21651.	21792.	21933.	22074.	22215.	22356.
21651.	21792.	21933.	22074.	22215.	22356.	22497.
21792.	21933.	22074.				

4609.	4623.	4636.	4649.	4663.	4676.	4689.	4703.	4716.	4730.	4743.	4757.	4770.	4784.	47
4824.	4838.	4852.	4865.	4879.	4893.	4906.	4920.	4934.	4947.	4961.	4975.	4989.	5003.	50
5044.	5058.	5072.	5086.	5100.	5114.	5128.	5142.	5156.	5171.	5185.	5199.	5213.	5227.	52
5270.	5284.	5298.	5313.	5327.	5341.	5356.	5370.	5385.	5399.	5414.	5428.	5443.	5457.	54
5501.	5516.	5530.	5545.	5560.	5574.	5589.	5604.	5619.	5634.	5648.	5663.	5678.	5693.	57
5738.	5753.	5768.	5783.	5798.	5814.	5829.	5844.	5859.	5874.	5890.	5905.	5920.	5935.	59
5982.	5997.	6013.	6028.	6044.	6059.	6075.	6090.	6106.	6122.	6137.	6153.	6169.	6184.	62
6232.	6248.	6264.	6280.	6296.	6312.	6328.	6344.	6360.	6376.	6392.	6408.	6424.	6441.	64
6489.	6506.	6522.	6538.	6555.	6571.	6588.	6604.	6621.	6638.	6654.	6671.	6687.	6704.	67
8610.	01573	8776.	90149	8058.	07850	6919.	38164	60933.	60933.	68768	43334.	33308	27333.	1.
68365		66359	72019	72019	83206	83206	90285	90285	90285	15.82225	15.82225	15.82225	12.362	12.
9.58423		7.91294	7.03068	7.03068	9.97572	9.97572	9.63306	9.63306	9.63306	47.0	47.0	47.0	47.0	47.
967.0		390.0	260.0	260.0	165.0	165.0	96.0	96.0	96.0	96.0	96.0	96.0	96.0	96.

END OF DATA

INITIAL DISTRIBUTION LIST

	No. Copies
1. LCDR P. Kalinyak, USN USS KEARSARGE (CVS 33) FPO San Francisco 96601	4
2. LT W. Danforth, USN USS BENNINGTON (CVS 20) FPO San Francisco 96601	4
3. Professor F. L. Martin Department of Meteorology & Oceanography Naval Postgraduate School Monterey, California 93940	3
4. Library Naval Postgraduate School Monterey, California 93940	2
5. Department of Meteorology & Oceanography Naval Postgraduate School Monterey, California 93940	3
6. Defense Documentation Center Cameron Station Alexandria, Virginia 22314	20
7. Naval Weather Service Command Washington Navy Yard Washington, D. C. 20390	1
8. Officer in Charge Naval Weather Research Facility Naval Air Station, Building R-48 Norfolk, Virginia 23511	1
9. Officer in Charge Fleet Numerical Weather Facility Naval Postgraduate School Monterey, California 93940	1
10. Commanding Officer U. S. Fleet Weather Central Box 110 FPO San Francisco 96601	1
11. Superintendent Naval Academy Annapolis, Maryland 21402	1

	No. Copies
12. Office of Naval Research Department of the Navy Washington, D. C. 20360	1
13. Department of Commerce, ESSA Weather Bureau Washington, D. C. 20235	2

Unclassified

Security Classification

DOCUMENT CONTROL DATA - R & D

(Security classification of title, body of abstract and indexing annotation must be entered when the overall report is classified)

1. ORIGINATING ACTIVITY (Corporate author)

Naval Postgraduate School
Monterey, California 93940

2a. REPORT SECURITY CLASSIFICATION

Unclassified

2b. GROUP

3. REPORT TITLE

A Six Level Prognostic-Diagnostic Solution Procedure with a New Approach in
Modeling of Boundary Layer Frictional Effects

4. DESCRIPTIVE NOTES (Type of report and, inclusive dates)

None

5. AUTHOR(S) (First name, middle initial, last name)

William Loynes Danforth and Paul Peter Kalinyak

6. REPORT DATE

June 1968

7a. TOTAL NO. OF PAGES

✓ 101

7b. NO. OF REFS

17

8a. CONTRACT OR GRANT NO.

b. PROJECT NO.

c.

d.

9a. ORIGINATOR'S REPORT NUMBER(S)

9b. OTHER REPORT NO(S) (Any other numbers that may be assigned
this report)

10. DISTRIBUTION STATEMENT

~~THIS DOCUMENT IS SUBJECT TO SPECIAL REPORTING AND IS NOT TO BE
REPRODUCED OR FORN DISSEMINATED IN ANY MANNER WITHOUT THE
APPROVAL OF THE NAVY POSTGRADUATE SCHOOL~~

11. SUPPLEMENTARY NOTES

12. SPONSORING MILITARY ACTIVITY

Naval Postgraduate School
Monterey, California 93940

13. ABSTRACT

A six-level baroclinic forecast model suitable for numerical prognosis was devised. This model includes vertical motion due to large-scale orographic and eddy-stress effects. The model was programmed in Fortran IV language, applied to a test case based upon initial data for 1200 GMT, 15 December 1967. A convergent 36-hour forecast was produced. Comparisons were made with the verifying analyses at 12-hour intervals.

14

KEY WORDS

LINK A

LINK B

LINK C

ROLE

WT

ROLE

WT

ROLE

WT

diagnostic omega equation

1

1

1

thesD1477

DUDLEY KNOX LIBRARY



3 2768 00422001 2

DUDLEY KNOX LIBRARY